UNCERTAINTY AND MODEL SENSITIVITY OF AGRICULTURE IRRIGATION ON ATMOSPHERIC LATENT HEATING

By

Molly Elizabeth Aufforth

A thesis submitted in partial fulfillment of

the requirements for the degree of

Master of Science

(Atmospheric and Oceanic Sciences)

at the

UNIVERSITY OF WISCONSIN—MADISON

2018

Abstract

The expansion and modernization of irrigation increased the relevance of knowing its feedback effects on regional weather and climate. This common agricultural practice cools surface temperatures (Alter et al., 2015; Im et al 2013), suppresses boundary layer height (Im et al 2013), increases low level moisture (Decker et al., 2017; Douglas et al., 2006), alters precipitation (Alter et al., 2015; Im et al 2013), and in some cases generates low level circulations (Alter et al., 2015; Im et al 2013). Being able to quantify these feedbacks is important for modeling ecosystem-atmosphere coupled systems. In this thesis, I seek to answer: Does the ecosystem model BioCro accurately predict the increase in latent heating (evapotranspiration) between irrigated and rain-fed cropland? Further, can this model be improved with observations? The model BioCro was evaluated for its ability to predict latent heat flux at a pair of eddy covariance flux tower sites in Nebraska, one irrigated and one rain-fed. I investigated model sensitivity of latent heating with respect to plant parameters for maize and the observed meteorology. The parameters stomatal slope, cuticular conductance, extinction coefficient for diffuse light, and leaf respiration rate added the most uncertainty to the model output of latent heating, with cuticular conductance and leaf respiration rate adding the most uncertainty after parameter data assimilation (PDA). Changing the air temperature by ±1 and ±2 °C did not modify model output of latent heating as much a change in the plant parameters. These parameters should be focused on for future field measurements. Observational analysis showed there was a significant difference in latent heat (LE), sensible heat (H), net radiation (RNET), soil temperature (TS), relative humidity (RH), soil water content (SWC), vapor pressure deficit (VPD), gross primary productivity (GPP), and net ecosystem exchange (NEE) between the two sites during the growing season. PDA slightly

improved the model results of latent heating near the end of the growing season for both sites, where results were still underestimated in the middle of the growing season. This could be from a misrepresentation of the phenology stage that effects evapotranspiration. Being able to further understand the impacts that irrigation has on land-atmosphere interactions should benefit farmers, ecologists, and atmospheric scientists alike. The connection between environments through the flow of water, carbon, and energy and how that system can be altered from an agricultural management decision will benefit our understanding of the system as a whole.

Table of Contents **Page**

Abstract i

Table of Contents iii

Acknowledgments v

Dedication vii

1. Introduction 1

2. Background 4

2.1 Irrigation and crop yield responses 4

2.2 Impacts of irrigation on the atmosphere 5

2.2.1 Temperature 5

2.2.2 Moisture 8

2.2.3 Convection and precipitation 9

2.3 Linkage of water, carbon, and energy 13

2.3.1 Water 13

2.3.2 Carbon 14

2.3.3 Energy 14

2.4 Ecosystem models 17

2.5 Sources of uncertainty in modeling 19

3. Methods 20

3.1 Data 20

3.2 Model 23

3.3 Informatics tool package 26

3.3.1 The Predictive Ecosystem Analyzer (PEcAn) 26

3.3.2 Database of plant traits and parameters 27

3.3.3 Modules included in PEcAn 29

4. Results 33

4.1 Observed impact of irrigation on LE 33

4.2 Impact of irrigation on local meteorology 35

4.3 Pre-PDA model BioCro response from irrigation 39

4.4 Post-PDA model BioCro response from irrigation 40

4.5 Model error 41

5. Discussion 43

5.1 Questions raised 43

5.2 Mechanisms of enhanced ET with irrigation 44

5.3 Comparison to other studies 45

5.4 Uncertainty and paths forwards 48

6. Conclusion 50

References 53

Figures 59

Tables 78

Acknowledgments

This work used eddy covariance data acquired and shared by the FLUXNET community, including these networks: AmeriFlux, AfriFlux, AsiaFlux, CarboAfrica, CarboEuropeIP, CarboItaly, CarboMont, ChinaFlux, Fluxnet-Canada, GreenGrass, ICOS, KoFlux, LBA, NECC, OzFlux-TERN, TCOS-Siberia, and USCCC. The ERA-Interim reanalysis data are provided by ECMWF and processed by LSCE. The FLUXNET eddy covariance data processing and harmonization was carried out by the European Fluxes Database Cluster, AmeriFlux Management Project, and Fluxdata project of FLUXNET, with the support of CDIAC and ICOS Ecosystem Thematic Center, and the OzFlux, ChinaFlux and AsiaFlux offices.

The following AmeriFlux sites were used for observational analysis: US-Ne2 year(s) 2001, 2003, 2005, 2007, 2009, 2011 (Andy Suyker, AmeriFlux US-Ne2 Mead - irrigated maize-soybean rotation site, doi:10.17190/AMF/1246085), and US-Ne3 years(s) 2001, 2003, 2005, 2007, 2009, 2011 (Andy Suyker, AmeriFlux US-Ne3 Mead - rainfed maize-soybean rotation site, doi:10.17190/AMF/1246086). For both sites, the year 2003 was used for model input. Funding for the individual sites was provided by the U.S. Department of Energy Office of Biological and Environmental Research & the Experimental Program to Stimulate Competitive Research. Funding for AmeriFlux data resources was provided by the U.S. Department of Energy's Office of Science.

The works for this thesis was supported by the National Science Foundation award number DBI-1457897.

I personally would like to thank everyone on the PEcAn team that helped me, especially Chris Black and Istem Fer for answering all of my modeling questions. I would

like to thank my committee members, Christopher Kucharik and Michael Notaro, for their helpful comments and suggestions for the advancement of this thesis. I would like to thank my fellow lab mates for inspiring me. I would like to thank my advisor, Ankur Desai, for guiding me through this whole process. A huge thanks to Kellen Peters, my mom, and the rest of my family and friends for their love, comfort, support, and words of encouragement given to me over the past two years I have spent in graduate school. Thank you all.

This thesis is dedicated to my dad.

1. Introduction

Humans need to consume food to live. Increasing crop yields and reducing current food waste is needed to feed a projected 9 billion people by the year 2050 (United Nations [UN], Department of Economic and Social Affairs [DESA], Population Division, 2017). The choices that farmers make impact harvest yields. To increase yields, farmers may irrigate their crops. Since the early 1900s, global area of irrigation has increased by nearly five times the amount since then (Rosegrant et al., 2002). In the United States, the top irrigated crop is corn, coming in at over 13 million acres (United States Department of Agriculture [USDA] National Agriculture Statistics Service [NASS], 2014). This study will focus on the specific feedbacks from the irrigation of corn.

Corn is a popular crop to produce because of its versatility. In 2010, a majority of corn was grown in midwestern U.S. (Figure 1). It can be grown for human consumption, livestock feed, biofuel, and other industry bioproducts. Having multiple beneficial services, there has been a growing debate on what corn should be grown for. Since there are many useful services that corn can supply, it has become important to optimize corn production to maximize yields while minimizing land area. When considering corn as a bioenergy crop, there is a broad agreement that it should be grown where irrigation is not required. The process to convert the harvested crop into a biofuel already has high water demands (Dale et al., 2010).

There are many different types of irrigation that include central pivot, surface drip, furrow, sub-surface, and many others. No matter what type, irrigation impacts the water, carbon, and energy cycles that alters the land-atmosphere system interaction. With noted

impacts on surface air temperature (TA), and low level moisture, there are other connected impacts on precipitation, evapotranspiration rate, planetary boundary layer (PBL) height, and others. Again, these impacts are important to both the water, carbon, and energy budgets.

Irrigation impacts the surface energy budget as more energy is partitioned towards LE than H. With water introduced to the air, soil, and crops through irrigation, there is more water available for ET, which impacts the partitioning of incoming energy. As a result, there is a notable cooling on surface air temperature. Irrigation introduces water to the system that otherwise would not be there naturally. The rapid expansion of irrigation in the United States has been shown from model results to induce a large cooling effect on summertime average daily daytime temperatures, specifically over California (Bonfils & Lobell, 2007).

Not only is the temperature decreased, the water budget is also impacted. Agriculture irrigation counts for ~85% of the global consumption of water withdrawals (Rosegrant et al., 2002). Irrigation not only impacts ground water, it also impacts precipitation amounts locally and remotely. A large-scale irrigation project known as the Gezira Scheme in the East African Sahel has decreased local rainfall over the irrigation area while it increased rainfall downwind as concluded from climatological observations and model results (Alter et al., 2015). Similarly, in a different study, increased irrigation over the Ogallala Aquifer in the Great Plains of the United States resulted in increased evapotranspiration which lead to precipitation increases downwind (DeAngelis et al., 2010).

This relationship between irrigation, soil moisture, evapotranspiration, and convection will affect the water cycle. There have been other studies that show different results when soil moisture is considered. One such study has suggested that convection can

either be suppressed or enhanced over irrigated areas depending on the preexisting soil moisture levels (Harding & Snyder, 2012). There is no doubt that irrigation affects the magnitude as well as the location of precipitation events.

The atmospheric carbon cycle has also been hypothesized to be affected by the practice of irrigation on agricultural fields. After accounting for the grain carbon harvested and the carbon dioxide (CO2) released from irrigation water, one study found that rain-fed maize–soybean rotation system is carbon neutral, irrigated continuous maize is nearly neutral or a slight source, and irrigated maize–soybean rotation is a moderate source of carbon (Verma et al., 2005).

However, these studies are often limited to observational studies and/or large-scale models that are poorly parameterized for small scale irrigated agricultural systems. I undertook a study to test model sensitivity of LE (evapotranspiration) to plant functional type (PFT) parameters associated with maize, sensitivity to atmospheric temperature, and the resulting uncertainties. I asked the following questions:

Can an ecosystem model accurately predict the increase in LE between irrigated and rain-fed cropland?

Can the model be improved with observations?

To address these questions, Section 2 describes the impacts of irrigation on crop yield the atmosphere, the link between water, carbon and energy, and ecosystem models and sources of uncertainty in ecosystem modeling. Section 3 includes the data, the specific ecosystem model, and other practices used to answer these questions. Section 4 covers the results from observational analysis and model output. Section 5 discusses these results and

compares it to similar previous studies to answer these questions. Finally, Section 6 provides the concluding remarks.

2. Background

2.1 Irrigation and crop yield responses

Irrigation is not solely responsible for increasing yields. With the 'Green Revolution', global crop yields increased from the distribution and advances in technology of crop genetics, fertilizers, methods of cultivation, modern machinery, irrigation, and others (Farmer, 1986). Looking at the future of crop yields without increasing irrigation, Bagley et al. (2012) found that land cover change effects on moisture availability could reduce crop yields and disrupt future food supplies.

The major way that irrigation increases yields is that it reduces water stress. More crops can be grown in relatively dry regions by using irrigation. The irrigated crops are less likely to be affected by a single year of climatic drought, and so annual variability of yield is not as strongly affected by mean annual precipitation. Irrigation can also regulate temperature by cooling on hot days as well as frost protection (Snyder & Melo-Abreu, 2005). The temperature regulation caused by irrigation reduces the variability of atmospheric temperature. The crop does not need to waste energy to regulate its own temperature but use that energy for grain production for example.

One study found that average global crop yields for irrigated cereals (wheat, maize, rice, barley, rye, millet, and sorghum) was 442 Mg km^{-2}, while the average yield of rain-fed cereals was only 266 Mg km^{-2} (Siebert & Doll, 2010). The authors also concluded that without irrigation, total cereal production would decrease by 20%. Crop yield ratio of rain-

fed to irrigated were based on the ratio between actual and potential crop evapotranspiration of rain-fed crops. Crop specific parameters were derived from a comparison of the observed yield ratios of rain-fed to irrigation to the actual and potential evapotranspiration ratios computed by the Global Crop Water Model (GCWM).

Under future climate predictions to the year 2050, Deryng et al. (2011) found that yields for irrigated maize increased a maximum of 6% globally according to present-day maize irrigated area when planting dates were adapted under the future climate conditions of temperature and precipitation. These results do not include consideration of future water availability nor the possible change in irrigated area. They used the global crop model Predicting Ecosystems Goods And Services Using Scenarios (PEGASUS) for their study.

Properly controlled irrigation promotes plant growth which impacts the ecosystem. There are also impacts of irrigation that affects the atmosphere. The next section will cover several studies that show irrigation reduces the local temperature.

2.2 Impacts of irrigation on the atmosphere

2.2.1 Temperature

There is overwhelming evidence showing that irrigation can affect the atmosphere. The most often reported is the cooling of surface temperatures. One of the earliest studies on the effect of irrigation in the U.S. Southern Great Plains was done by Barnston and Schickedanz (1984). They showed that irrigation lowered the daily maximum surface temperature by 1.7-2.8°C, lowered daily minimum temperature by 0.5°C, and the resulting diurnal temperature range reduced by 1-2°C. Bonfils and Lobell (2007) concluded that irrigation had negligible effects on nighttime temperatures and that cooling of surface

temperatures was more notable during the daytime. The asymmetrical impact of irrigation at the diurnal timescale can partly be explained by the surplus of energy at the surface to partition into LE and H and the active transpiration of plants during the daytime.

Adegoke et al. (2003) looked at both model results and observations. They conducted a statistical analysis of long-term (1921-2000) surface temperature from irrigated and non-irrigated sites in Nebraska. They found that the growing season monthly mean maximum temperature for the irrigated site showed a steady decreasing trend, while the non-irrigated site showed an increasing trend. Using the Colorado State University Regional Atmospheric Modeling System (RAMS) model for four different land cover scenarios, they confirmed the irrigational cooling effect in near-ground temperatures.

A more recent study by Harding and Snyder (2012), utilized the satellite derived product from Ozdogan and Gutman (2008) of irrigated land specifically for the U.S. Great Plains (Figure 2). They showed that with the decrease in H over much of the U.S. Great Plains from irrigation lead to a decrease in 2-m temperature (Figure 3). They used the Weather Research and Forecasting (WRF) model version 3.2 to simulate the atmospheric response to irrigation coupled to the Noah Land Surface Model (LSM) which provides surface fluxes of energy, momentum, and mass that includes a vegetation component. Irrigation was represented from the 500-m resolution Moderate Resolution Imaging Spectroradiometer (MODIS) derived fraction irrigation dataset from Ozdogan and Gutman (2008).

Several studies looked at irrigation outside of the United States. Using the Massachusetts Institute of Technology regional climate model (MRCM), Im et al. (2013)

found that large scale irrigation in West Africa induced surface cooling. Also using the MRCM and climatological observations over the Gezira irrigation scheme in East Africa, Alter et al. (2015) also found similar results. They found that the rapid intensification of irrigation during the 1960s has led to localized cooling. Douglas et al. (2009) showed a decrease in air temperature by 1 to 2°C from irrigation in India.

When evaluating the effect of irrigation on near surface temperature of the areas surrounding the irrigation, Decker et al. (2017) showed that irrigation did not significantly impact the maximum temperature during the growing season in East Australia. They used the National Aeronautics and Space Administration (NASA) Unified WRF (NU-WRF) model coupled to the Community Atmosphere Biosphere Land Exchange (CABLE) land surface model. The change in mean temperature limited to the regions of irrigation did show a statistically significant decrease.

Bright et al. (2017) showed that changing from rain-fed crops to irrigated crops across the globe led to cooling over the local areas. They combined predictions from a semi-mechanistic empirical model with satellite remote sensing and other global observations to get global estimates of the local temperature responses from the land cover management change (LCMC) from rain-fed to irrigated crops and eight other different changes.

There is no doubt that these cooling effects occur on a local scale. Bonfils and Lobell (2007) noted that the impacts on temperature are not expected to influence broad regions, only local. These regional impacts depend on the wind advection of moisture in the air. Observing these temperature changes over longer temporal and larger spatial scales, irrigation does not change the temperature significantly as the water that does evaporate

eventually condenses balancing out any local perturbations in the energy budget (Pielke et al., 2002). The partitioning of energy is not the only factor impacting temperature. The amount of available incoming energy also impacts temperature.

The surface temperature also depends on the surface albedo. Albedo decreases with the increasing darkness of moist soils. Eltahir (1998) noted this effect that the darker and wetter soils decreased the surface albedo which implies that wet soil conditions enhance net solar radiation. This could lead to an increase in surface air temperature. With the previous studies showing that the temperature decreases from irrigation, it is reasonable to conclude that the influence of evaporation of water on temperature outweighs any change to the surface albedo. This change in albedo could possibly explain some of the differences in magnitude of temperature decreases among the different studies.

2.2.2 Moisture

While temperature effects can be complex, the effect of irrigation on local near surface atmospheric moisture is relatively straight forward, though downstream regional effects are less well quantified. As moisture is introduced to the atmosphere near the surface through irrigation, surface moisture increases. This would increase humidity, dew point, mixing ratio, soil water content, and other variables representing moisture in the atmosphere and soil.

Harding and Snyder (2012) showed that with the increased LE, there was an increase in 2-m mixing ratio as well over the region of irrigation (Figure 3). Limited to 20 m above the surface, relative humidity increased by 25% as set by Barnston and Schickedanz (1984) from the increase in moisture and decrease in temperature. Irrigation increased specific

humidity by 5-10% (Decker et al., 2017). Water vapor fluxes increased 17% from pre-agriculture land cover to irrigated contemporary agriculture land cover across India (Douglas et al., 2006).

Irrigation introduces water to the air as it evaporates as well as liquid water to the surface soils. Im et al. (2013) noted that an increase in soil moisture enhances evapotranspiration, resulting in a higher moisture flux and moist static energy in the PBL. The moisture concentration within the entire PBL depends on the development of the PBL through surface daytime heating which can lead to convection. The changes in surface temperature and moisture content have further implications and feedbacks that impact convection and precipitation.

2.2.3 Convection and precipitation

The effect of local moisture advected downstream plays a role in the development or suppression of convection and resulting precipitation. Decreasing local temperature and increasing moisture work against each other when considering how convection is impacted by irrigation. The decrease in surface temperature alters the environmental lapse rate to be more stable, but the increase in moisture near the surface would decrease the height of cloud formation. Surface based parcels would not have to rise as much to become saturated when surface moisture increases. Once convective clouds develop, then precipitation can occur. The feedback of irrigation on precipitation occurs locally and remotely. These highly depend on how the what generates the convection and the advection of the low level moisture.

Locally, the impacts of temperature and moisture affect the PBL height. The PBL height has been reported to be proportional to H (Douglas et al., 2006). Using RAMS model

version 4.3 and the Global Land Cover 2000 (GLC2000) dataset, Douglas et al. (2009) showed a decrease in PBL height from 2800 m in the potential pre-agriculture land cover case to 2100 m when irrigated cropland was considered. Other studies have also shown that the local PBL to decrease (Im et al., 2013).

Harding and Snyder (2012) showed that there was a decrease in the PBL height over the irrigated regions in the domain of their study (Figure 4). Along with the change in the PBL height, there was a notable increase in convective available potential energy (CAPE) with no significant change in convective inhibition (CIN) over the irrigated region. There was an increase in column precipitable water, but not directly over the irrigated region.

Any local convection highly depends on if the PBL is unstable. In an early study done by Barnston and Schickedanz (1984), they showed that the lifted index decreased by one from the effect of irrigation. The hypothetical sounding produced for their study showed that with the effect of irrigation that the dew point temperature increased while the temperature decreased (Figure 5). Even without surface convergence, the temperature and dew point anomalies increased instability therefore slightly increasing the probability for convection. Even though the lapse rate immediately above the surface declined, the fact that the additional moisture lowered the liquid condensation level (LCL) leading to a lower level of free convection (LFC) means the instability can increase above that point in the atmosphere while the surface lapse rate declined.

Looking at remote impacts of irrigation on convection and precipitation, one must look at larger temporal and spatial scale impacts to mesoscale circulation patterns and synoptic sized disturbances. It has been found that during the wheat growing season in

Australia, precipitation events are not determined by localized convection, but rather synoptic events that are not as strongly influenced by irrigational effects (Decker et al., 2017). Douglas et al. (2009) reported that if the irrigation area was large enough (10s of km or larger), then mesoscale circulations can develop.

Anti-cyclonic circulations have generated by being induced from surface cooling, which then leads to localized subsidence that generates these anomalous wind patterns impacting regional convection and precipitation (Im et al., 2013; Alter et al. 2015). Im et al. (2013) showed that the remote location for enhanced precipitation in western Africa highly depends on the latitudinal location of the irrigated region, timing and amount of supplied irrigation water, and how it interacts with the West African Monsoon. Over the irrigated area itself, there was a consistent pattern of decreased rainfall in all simulations. They noted that the magnitude of the decrease in precipitation seemed proportional to the rainfall climatology of each irrigated area. Alter et al. (2015) had similar findings where the anomalous low-level circulation pattern interacted with the background prevailing wind direction leading to horizontal convergence east of the irrigated area. This then lead to upward vertical motion and increased rainfall remotely.

With irrigation inducing mesoscale circulations, it has been questioned whether it can lead to increased convection and rainfall. DeAngelis et al. (2010) looked at irrigation intensification via ground water withdrawal after World War II over the Ogallala Aquifer in the Great Plains of the United States. Evaluating long term observations of precipitation and wind for vapor transport analysis with simulations of a General Circulation Climate Model (GCM), they did find an increase in precipitation from 15 – 30% from the eastern most part

of the aquifer and further downwind. They mentioned that there was no clear evidence that changes in the atmospheric circulation lead to the increase in precipitation.

A more recent study by Lu et al. (2017) found a consistent and significant decline in the local coupling strength of the irrigated land to the atmosphere in the Midwest and northern Great Plains of the United States. They used a regional climate model (WRF3.3) that incorporated dynamic crop growth and precision irrigation (CLM4crop). They found that this reduction in coupling strength was due to increased soil moisture but decreased local precipitation and lower sensitivity of LE to soil moisture over the irrigated regions. Water vapor from the irrigated land was transported to the Midwest and to the northeastern part of the U.S. which suggests that irrigation has a broader spatial impact on soil moisture-precipitation feedbacks than simply through local soil moisture-evapotranspiration coupling. Results from this study suggest that climate models, without irrigation schemes, may overestimate the coupling strength over the local irrigated regions but underestimate it over the rain-fed neighboring areas.

With multiple studies suggesting that that irrigation impacts convection and precipitation, the main question becomes whether how strong the connection was between the land and atmosphere over the local and remote regions. These conclusions highly depend on the spatial scale of the irrigated region as well as the regional dynamic effects. It is also highly dependent on which processes of cooling and/or moistening has the dominant effect for an individual case or region.

Irrigation impacts the atmosphere as all these studies mentioned previously contributed plenty of evidence to confirm the many different impacts. Now we will look

closer to the surface at the plant level interaction between the atmosphere with the water, carbon, and energy cycles.

2.3 Linkage of water, carbon, and energy

2.3.1 Water

Understanding how to predict the effect of irrigation on the atmosphere requires understanding how plants use water, carbon, and energy. Water is the main constituent of most plant cells (Nobel, 1974). It supports the structure of the plant itself. For example, a peace lily will begin to wilt if it lacks water. Once the plant does obtain water, its structural integrity returns. The stems and leaves gain enough strength to stand back up. Other than supporting the plants structure, the water molecule is stripped of an electron during the photosynthetic process and then transpired. Specifically, for this research it is important to note that corn is a highly transpiring crop as a single acre of corn can transpire 3,000 to 4,000 gallons of water in a day (United States Department of the Interior, U.S. Geological Survey [USGS], 2016). This is because it is highly productive, the plant must use lots of water to keep up with the high production rates. During the growing season, about 100 times more water is transpired by a plant than remains in it (Nobel, 1974).

Mentioned previously about irrigational water regulating temperature, plants use their own water for temperature regulation. Plants can regulate temperature by opening their stomata to transpire water, which enhances evaporation that cools off the leaves in hot environments (Jones & Rotenberg, 2011). This is because temperature strongly regulates canopy assimilation rate. For C4 species, the optimum temperatures for photosynthesis are

higher than C3 and crassulacean acid metabolism (CAM) species (Yamori et al. 2014). The optimal air temperature range for corn is from 10°C to 30°C.

2.3.2 Carbon

When sun light and temperature are not limiting, the rate of photosynthesis in plants is generally limited by the amount of CO2 (Nobel, 1974). Corn, a C4 crop, is already saturated under current CO2 levels. Under current conditions, CO2 should not be a limiting factor for photosynthesis or canopy assimilation. There has been some speculation on what elevated CO2 concentrations predicted for the future could mean for all plant types. A Free-Air Concentration Enrichment (FACE) study during the 2004 growing season for corn showed that with the absence of water stress, growth at elevated CO2 concentrations did not stimulate photosynthesis (Leakey et al., 2006). The authors did show that under the elevated conditions, stomatal conductance was lower and soil moisture was higher. This makes sense as the stomata does not need to be open as much to take in CO2, and that leads to less water vapor being transpired. With less water transpiring, more water remains available in the soil.

2.3.3 Energy

The link between water, carbon, and energy is photosynthesis. The ultimate source of energy is the sun. The first step in the utilization of sunlight is the conversion of its radiant energy into various forms of chemical energy by the primary process of photosynthesis (Nobel, 1974). Plants use this energy to create carbohydrates from CO2 and water. This can be explained in the chemical formula of

$$6CO_2 + 6H_2O + light\ energy = C_6H_{12}O_2 + 6O_2\ .$$

In the light harvesting process, only a fraction of the sun's energy could be used in photosynthesis (Nobel, 1974). This fraction is known as photosynthetic active radiation (PAR) which is the designated spectral range from 0.4 μm to 0.7 μm within the solar radiation spectrum that plants can harvest energy from. This is more commonly known as the visible wave band.

Plants are not perfectly efficient at absorbing the PAR, they can only take a small fraction of this absorbed energy. This is called the Fraction of Absorbed Photosynthetically Active Radiation (FAPAR). This fraction of absorbed radiation links the flow of energy through the biosphere to the consumers. Photosynthesis is necessary for life to prosper (Nobel,1974). Water, CO2, temperature, light and other factors can limit the rate of photosynthesis. The rate of this process is what determines the feedbacks that impact the atmosphere.

The photosynthetic pathway differs between plants. Mentioned previously, there are three main different categories which include C3, C4, and CAM. There are approximately 85% C3 species, 5% C4 species, and 10% CAM species representing of all vascular plant species (Yamori et al. 2014). Vascular plants are defined as a plant that is characterized by the presence of conducting tissue. This paper focuses on maize, which is a C4 plant. This means that the light dependent reactions and the Calvin cycle are separated spatially in the mesophyll and bundle-sheath cells respectively (Hatch & Slack, 1968).

For C4 photosynthetic pathway, atmospheric CO2 enters through the open stomata and is then fixed to phosphoenolpyruvate (PEP) during carboxylation in the mesophyll cell forming a 4-carbon organic acid called oxaloacetate (OAA). For maize specifically, the CO2

is fixed by the specific Ribulose-1,5-Bisphosphate Carboxylase/Oxygenase (RuBisCO) enzyme nicotinamide adenine dinucleotide phosphate malic enzyme (NADP-ME) (Yamori et al., 2014). The OAA is then converted to malate which can be transported to the bundle-sheath cell. Then the malate breaks down during decarboxylation releasing CO2 and pyruvate. The Calvin cycle takes over, where chemical reactions occur to produce sugars from the released CO2. Adenosine triphosphate (ATP) must be expended to return the 3-carbon pyruvate molecule from the bundle-sheath cell to the mesophyll cell to make PEP that can pick up more atmospheric CO2, continuing the photosynthetic process.

The major parameter in the photosynthetic process that affects water vapor and carbon fluxes is the stomatal conductance. The plant stomata are the main channels that the exchanges of water vapor and CO2 occur between the plant and the atmosphere. Grasses such as oats barley, wheat, and corn all have approximately equal distribution of stomata on both sides of the leaves (Nobel, 1974). Stomata opening is controlled by many factors including concentration of CO2, light intensity, and water supply (Srivastava & Singh, 1972). The connection between water, carbon, and energy is a complex process that occurs on a small scale. The larger scale partitioning of energy also has its challenges.

The energy balance closure problem of eddy covariance measurement techniques is that the observed net radiation was greater than the measured heat fluxes of sensible, latent, and ground heat. The excess or residual energy must be used somewhere. It has been suggested that the energy balance closure problem results from instrumental errors, neglecting energy storage, loss of low frequency components in the flux-averaging procedure, and heterogeneities in the surrounding areas (Jacobs et al., 2008). A closer of

96% was obtained by computing all possible enthalpy changes of LE, H, ground heating, canopy storage, and photosynthesis, where photosynthesis can be approximated from 1 mg CO_2 m^{-2} s^{-1} canopy assimilation equal to 11 W m^{-2} (Nobel, 1974; Meyers & Hollinger, 2004), and using the harmonic analysis technique for surface soil heat flux (Jacobs et al., 2008). Although, Foken (2008) suggested that neither measurement errors, when measurements are carefully done, nor storage terms significantly impact the residual energy. Instead, the greatest influence on energy budget closure is from the exchange processes that occur on larger scales over heterogeneous areas. The fact that irrigation strongly affects the partitioning of the two major heating fluxes and that it adds heterogeneity to the agricultural landscape increases the need to study and model the effects of irrigation.

2.4 Ecosystem models

There are many plant parameters and environmental factors that go into the fluxes of water, carbon, and energy exchange. The main issue is how to represent these physical processes mathematically in ecosystem models. Models that are not ecosystem models, such as land-atmosphere coupled models, lack in capturing the physical processes that represent crop dynamics, biogeochemical interactions, and water and energy flows through crops into the surface (Bagley et al., 2014). That is why it is important to use ecosystem models when investigating the impact of irrigation of agricultural crops.

For the SiBcrop model, the same five sites mentioned in the previously mentioned study were evaluated with the model performance with a newly developed phenology and physiology scheme (Lokupitiya et al., 2009). The authors concluded that leaf area index (LAI) and NEE values produced by SiBcrop for maize were closer in value to the observed

field data compared to the original SiB model which LAI was based on the remotely sensed Normalized Difference Vegetation Index (NDVI). Especially for maize, they found that SiBcrop better predicted planting dates and crop growth which improved the estimate of CO2 uptake.

Another ecosystem model that predicts agricultural crop growth includes Agro-IBIS. This model is an updated U.S. agricultural version of the (Integrated Biosphere Simulator) IBIS model. With respect to maize crop yields across the U.S. corn belt, the model results were tested for its sensitivity to hybrid selection, planting date, and soil type (Kucharik, 2003). In conclusion, the spatial patterns of simulated crop yield were largely unresponsive there was a weak response of yield to changes in soil texture, optimum hybrid choice, and planting dates for the U.S. Corn Belt. The author also noted that the impacts of irrigation on maize yields must be properly accounted for in future modeling studies to capture increases in productivity, water usage, and decreased interannual variability compared to rain-fed maize.

For this study, it was important to pick an agricultural ecosystem model that has specific parameterizations for the crop specific plant functional type of maize. One model that was not included in the Lokupitiya et al., (2016) study that was used for this study was BioCro. To study the impacts of irrigation, the same sites of US-Ne2 and US-Ne3 used in Lokupitiya et al., (2016) were also used in this study. More discussion of the specific plant parameters, model, and study sites will be covered in section three.

2.5 Sources of uncertainty in modeling

As mentioned previously, land surface heterogeneities such as agricultural irrigation add uncertainty to model results. Uncertainty in model results from any type of numerical model is impossible to avoid. With current computing power, the models cannot fully capture the complex processes of the ecosystems from the tinniest cells and scaled up to full forested canopies. It also limits our understanding of the physical processes. That is why it is important to pay attention to uncertainty.

There are several sources of uncertainty with modeling ecosystems. Uncertainty can come from measurement error of observed conditions, unknown future conditions, model specification of processes, and parameters represented in those processes (McMahon et al., 2009). Observational uncertainty depends on the instrumentation itself. Jacobs et al. (2008) also noted that the observations using the eddy covariance (EC) technique of LE and H were not measured well during low wind conditions. Understanding what factors affect predictability directly impacts what data to collect, how models are structure, and the statistical tools used to link models to data (Dietze, 2017).

From equation two in Dietze (2017), the uncertainty in model prediction can be quantified in terms of variance in the prediction. The variance in prediction depends on initial condition (IC) uncertainty, IC sensitivity, driver sensitivity, driver uncertainty, parameter sensitivity, parameter uncertainty, parameter variability, and process error. Providing an example of predicting NEE at a single site, the author concluded that in contribution to the forecast uncertainty, initial condition uncertainty dissipated rapidly over the time of interest, parameter and driver uncertainties both contributed moderately, and the forecast was

dominated by process error. For cumulative NEE, parameter uncertainty dominated in contribution to the forecast uncertainty.

Knowing that irrigation impacts both the atmosphere and surface biology is motivation enough to study these impacts using ecosystem models that best represent the physical processes that influence water, carbon and energy. Then by understanding these processes and what drives the uncertainty in model results the motivating questions can be answered. The following section follows what tools and methods I used to answer these questions.

3. Methods

3.1 Data

The study site at the University of Nebraska Agricultural Research and Development Center near Mead, Nebraska part of the FLUXNET network of AmeriFlux was used for this project. These sites are large agricultural production fields approximately a quarter of a square mile in size. The sites US-Ne1 (41.1651°N, 96.4766°W, 361 m), US-Ne2 (41.1649°N, 96.4701°W, 362 m), and US-Ne3 (41.1797°N, 96.4397°W, 363 m) are located within 1.6 km of each other and southeast of Mead, Nebraska. The sites US-Ne1 and US-Ne2 are irrigated by a center pivot irrigation system while US-Ne3 is naturally rain-fed. These sites are part of a research program that focuses on understanding the differences in carbon sequestration between irrigated and rain-fed corn (Suyker et al., 2004). Before the initiation of the study in 2001 all sites had a 10-year history of maize-soybean rotation under no-till management. Since then, US-Ne1 is seeded with maize year after year while the other two sites rotate between maize and soybean. At all the sites, corn was grown for the years 2001, 2003, 2005,

2007, 2009, 2011, and 2013. The sites US-Ne2 and US-Ne3 were soybean for the even years in between.

Before the study began, all sites were tilled via disking to homogenize the top 0.1 m of soil and incorporate phosphorus fertilizers, potassium fertilizers, and other accumulated surface residues. The sites have been under no-till management since then. But after the 2005 harvest, the US-Ne1 site was tilled under conservation-plow operation and a small amount of nitrogen fertilizer was sprayed on the residue immediately prior to the plow operation. Approximately 33% of the crop residue was left on the surface. This post-harvest conservation-plow operation has continued since the 2005 harvest. All sites follow best management practices for fertilizer and pesticide applications. The soil texture at US-Ne1 is 11%, 52%, and 37% of sand, silt, and clay respectively with similar ratios at US-Ne2 (12%, 55%, 33%) and US-Ne3 (8%, 57%, 35%).

For simplicity, US-Ne2 and US-Ne3 will be the focus for this study to minimize any biases of the measured observations since the follow the same crop rotation. US-Ne2 is the irrigated site closest to the rain-fed site. For this thesis, the observational analysis will include the years 2001, 2003, 2005, 2007, 2009, and 2011 and a focus on the year 2003 for model analysis. The years were selected on the basis that corn was grown at both sites. For the year 2001, measurements began a few weeks after planting and continued for the rest of the study. The year 2013 was a corn growing year, but he measurements ended on June 1st, which is why it was not included for the observational analysis.

The EC technique (Baldocchi et al., 1988) was used to continuously measure the fluxes. The general idea of the EC technique is that horizontal air flow contains numerous

rotating eddies. Each eddy has unique horizontal motions, vertical motions, temperature, pressure, humidity, and gas concentrations. The net vertical eddy flux of a gaseous concentration under question can be determined by averaging the high frequency measured perturbations of the above listed parameters. To have enough fetch in all directions representative of the corn field, the EC sensors were mounted 3.0 m above the ground when the canopy was shorter than 1 m, and later moved to a height of 6.0 m until harvest. To measure the fluxes of CO2, water vapor, sensible heat, and momentum, the following sensors were used: an omnidirectional 3D sonic anemometer (Model R3: Gill Instruments Ltd., Lymington, UK), a closed-path infrared CO2/H2O gas analyzing system (Model LI6262: Li-Cor Inc., Lincoln, NE), and a krypton hygrometer (Model KH20: Campbell Scientific, Logan, UT) (Verma et al., 2005).

Data gaps were filled via the marginal distribution sampling (MDS) method and/or European Reanalysis Interim (ERA-Interim) data already provided from the AmeriFlux/FLUXNET network. The MDS gap filling method considers both the covariation of fluxes with meteorological variables and the temporal auto-correlation of the fluxes (Reichstein et al., 2005). The meteorological input variables for the model include the hourly observations of net radiation, air temperature, relative humidity, wind speed, and precipitation. For the chosen year of 2003, there was approximately 3.93% of the input that had missing data at the irrigated site US-Ne2. There was no missing data for wind speed, relative humidity, or precipitation. As for net radiation, that counted nearly 0.11% of the missing data and the remaining was missing from air temperature. All but 20 hours were missing after August 21st, which is in the later part of the growing season. For the rain-fed

site US-Ne3, there was nearly 4.9% of the input data that was missing. There was no missing data for wind speed or precipitation, but there was less than 0.1% missing in net radiation and nearly 0.5% missing from relative humidity, which were all before May 30th. Like US-Ne2, most of the missing data points for US-Ne3 was air temperature with almost 0.2% occurring before August 14th. The remaining majority was missing in air temperature after that date.

3.2 Model

To further understand the observational differences between US-Ne2 and US-Ne3, model output from each site was also analyzed. The model used for this study, Bioenergy Crop model (BioCro), was based from the ideas developed in the Windows Intuitive Model of Vegetation response to Atmosphere and Climate Change (WIMOVAC) (Humphries & Long, 1995). The WIMOVAC model was designed to simplify the modelling of various aspects of plant photosynthesis with emphasis on the effects of global climate change. Previously, BioCro has been used for predicting biomass yield and leaf area index of switch grass and miscanthus (Miguez et al., 2009).

BioCro is an ecosystem model that predicts plant growth over time given hourly observations for net radiation, air temperature, relative humidity, wind speed, and precipitation as input. The way that the model handles irrigation is by the precipitation input amount. The precipitation at US-Ne3 is strictly rain fall while the precipitation values at US-Ne2 include irrigation and rain fall. The irrigational occurrences spanned over ~2-3 hours. As for the soil texture, the model was set with a silty clay loam soil type which is made up of 9%, 58% 33% of sand, silt, and clay respectively that closely represents the soil texture measured at the sites.

The area of soil that is exposed to direct solar radiation is a function of LAI. This does not consider agricultural tillage. Previous studies have shown that the amount of residue left on the surface between growing seasons affects the temperature and the rate of soil evaporation as it acts as an additional non-living canopy (Kucharik & Twine, 2007). The model currently sets the soil temperature as the air temperature, which impacts the evaporation rate. It is important to know what other parameters are important in calculating the evapotranspiration and latent heat flux.

As mentioned earlier, plants control the flow of water, carbon, and energy between the atmosphere and land surface. The model BioCro uses the C4 photosynthesis model of Collatz et al. (1992). Where the net rate of photosynthesis (A_n) is simplified as

$$A_n \sim min \begin{Bmatrix} J_i, & f(\alpha, Q_p) \\ J_c, & g(p_i, k, T_l) \\ J_e, & h(V_{cmax}, T_l) \end{Bmatrix} - R_d \ ,$$

where T_l is leaf temperature, and α is the product of leaf absorptance and the intrinsic quantum utilization efficiency. J_i is the light dependent rate as a function of α and the incident quantum flux density (Q_p). J_c is the CO2 limited flux as a function of intercellular CO2 partial pressure (p_i), k is a pseudo-first order rate constant for PEP carboxylase, and T_l. J_e is the rate that is largely independent of CO2 and light. This was based off previous work from Farquhar et al. (1980) for C3 photosynthesis.

BioCro uses the Ball-Berry model for stomatal conductance. Ball et al. (1987) developed the following equation for stomatal conductance (g_s) calculated from CO2 assimilation (A), relative humidity at the leaf surface (h_s), mole fraction of CO2 at the leaf surface (c_s), where m and b are the stomatal slope and intercept (cuticular conductance)

obtained by linear regression analysis from data from gas exchange measurements of plant leaves represented in the equation

$$g_s = m \frac{A\, h_s}{c_a} + b \ .$$

The stomatal conductance and photosynthesis impact latent heating. Latent heating was not one of the original model outputs. It was calculated from the model output of soil evaporation (Evap) and vegetation transpiration (TVeg), which was calculated in W m^{-2} in the equation

$$LE = (Evap + TVeg) * Lv \ ,$$

Where Lv is latent heat of vaporization. Evap is a function of leaf area index, air temperature, incident radiation, available water content, field capacity, wilting point, wind speed, and relative humidity. TVeg is a function of A_n. Lv was calculated in the equation

$$Lv = 2500.8 - 2.36T + 0.0016T^2 - 0.00006T^3 \ ,$$

where T is the observed air temperature in °C. and Lv is in units of J g^{-1}.

Nitrogen cycling in agricultural systems is another important part of plant growth, especially for corn as it depletes nitrogen from the soils. That is why in most agricultural systems rotate every year between growing corn or soybeans. This is another reason why US-Ne1 was not used in this study as it is a continuous corn growing site, while the other two rotate between corn and soybeans. Within the model, nitrogen parameters can be prescribed to the model, but they were not required for the model to successfully run and were not included in this study.

3.3 Informatics tool package

3.3.1 The Predictive Ecosystem Analyzer (PEcAn)

To analyze the differences in observed and modeled LE between US-Ne2 and US-Ne3, PEcAn was used for this thesis. It is not a model itself, but a tool used to manage the flow of information for ecosystem modeling (LeBauer et al., 2013) (Figure 6). It consists of an application program interface that encapsulates an ecosystem model (Figure 6 orange box), providing a common interface, inputs, and output. The goal of using this product is to streamline the modeling information by tracking, processing, and synthesizing data and model output. This should make the development and application of ecological data and models more accessible, transparent, and relevant. PEcAn accomplishes two goals: first, it synthesizes data and propagates uncertainty through an ecosystem model; second, it places an information value on subsequent data collection to efficiently reduce uncertainty. Because of these goals and the included access to the model BioCro, that is why this package was used for this work. There are other models included in the software package of PEcAn.

Models in PEcAn currently includes BioCro, Community Land Model (CLM), Data Assimilation Linked Ecosystem Carbon model (DALEC), Ecosystem Demography Biosphere model (ED2), Functionally-Assembled Terrestrial Ecosystem Simulator (FATES), Generic Decomposition and Yield model (GDAY), LINKAGES, Lund-Potsdam-Jena General Ecosystem Simulator model (LPJ-GUESS), Simplified Photosynthesis-EvapoTranspiration model (SIPNET), Multiple-array Assimilation Evaporation Soil Plant Atmosphere model (MAESPA), and PREdict with Large Eddy Simulations model (PRELES) (“The Predictive Ecosystem Analyzer,” 2018). Choosing which model to use was simple as

BioCro was specifically developed for crop ecosystems unlike the other ecosystem models already available within PEcAn. Available meteorological drivers (Figure 6 blue box) include AmeriFlux, FLUXNET, NARR, CRUNCEP, CMIP5, NLDAS, GLDAS, PalEON, and Geostreams.

3.3.2 Database of plant traits and parameters

PEcAn queries the Biofuel Ecophysiological Traits and Yields Database (BETYdb) for specific parameters of species-level data (Figure 6 purple box) of prior trait distributions. BETYdb is a database of plant traits and parameters, that can be used for research, forecasting, and decision making (LeBauer et al., 2010). The purpose of this database is to provide users with data that has been collected from research projects in a consistent format in a user-friendly interface. Bayesian methods provide probability distributions as their output from the plant parameters from the database (Dietze et al., 2013) (Figure 6 prior white box). . The priors are traits and parameters for specific PFTs such as maize, miscanthus, switchgrass, and many others. Then meta-analysis (Figure 6 meta-analysis red box) was used to calculate the posterior values (Figure 6 posterior white box) used in the ecosystem model. In the database for the needed priors, there was only one observation of stomatal slope and 16 observations of quantum efficiency specifically for corn that were used in the meta-analysis

The parameters used for this project are shown in Table 1 as concluded after meta-analysis which includes the parameters, distribution type, and for each distribution type the columns A and B, in the parameters respective units, represent mean and standard deviation respectively for the normal and log normal distributions, shape and scale parameters

respectively for the gamma and Weibull distributions, and the first and second shape parameters respectively for the beta distribution. The column N represents the number of observations. Phylogeny is the group of plants that the trait was observed for. These categories are acceptable to use for modeling corn, because it is a plant, graminoid (an herbaceous plant with a grass-like morphology), tropical grass, and monocot (short for monocotyledon that is a flowering plant with and embryo that bears a single seed leaf). The last column is the source where the observations originally came from.

The following plant parameters in Table 1 are described as follows. The carbon to nitrogen (C:N) is the ratio of those two elements present in the plant's leaves. The cuticular conductance, when the stomata are fully closed, is the intercept for the Ball-Berry model for stomatal conductance. Extinction coefficient for diffuse light is represented by k_d in BioCro in the equation

$$I_{diffuse} = I_{diff} e^{-k_d CumLAI} + I_{scat} ,$$

where $I_{diffuse}$ represents the amount of light that is available within the canopy layer that is also dependent on the incoming diffuse sunlight (I_{diff}), cumulative leaf area index (CumLAI), and the incoming scattered sunlight (I_{scat}). Growth respiration coefficient is the amount of CO2 released due to growth per unit net photosynthesis. Leaf angle distribution is the ratio of projected area to hemi-surface area for an ellipsoid vertical which is represented as chi.l in BioCro. Leaf respiration rate is represented by R_d as the rate of CO2 release. Quantum efficiency is the efficiency with which light is converted into fixed carbon. Specific leaf area is the ratio of leaf area to dry mass. Stomatal slope is the slope in the Ball-Berry model for

stomatal conductance. Finally, V_{cmax} is the maximum rate of carboxylation, which determines the photosynthetic capacity along with the limitation of the electron transport rate (J_{max}).

3.3.3 Modules included in PEcAn

The PEcAn workflow includes modules for model parameterization, error propagation, and analysis. There is an extensive collection of modules to handle specific types of analyses (sensitivity, uncertainty, ensemble) model-data syntheses (benchmarking, parameter data assimilation, state data assimilation), and data processing (model inputs and data constraints) ("The Predictive Ecosystem Analyzer," 2018). For this thesis, modules used included ensemble analysis, sensitivity analysis, uncertainty analysis, and model-data combination parameter data assimilation (Figure 6 red boxes).

Ensemble analysis involves repeating numerous runs, which was 1000 for this project. Each run samples from the parameter uncertainty to generate a probability distribution of model projections. From this a confidence interval that reflects the current uncertainty of all model parameters can be determined on the model.

Sensitivity analysis is used to understand how much a change in a model parameter affects model output (LeBauer et al., 2013). This entails repeating numerous model runs used to assess how changes in model parameters affect the model outputs. This is used to identify which parameter the model is most sensitive to. The parameter distributions as previously described in Table 1 were used for this analysis with respect to change the model output of LE. This process included varying the parameters over 1000 model iterations by ±1 and ±2 standard deviation(s) as determined from the mean value from their respective density functions.

Combining results from the sensitivity analysis with information about the model parameter uncertainty then it can be determined how much uncertainty each parameter contributes to the model output uncertainty. This process is shown as variance decomposition in Figure 6 (red box). This project specifically looked at the uncertainty contributed from each parameter with respect to LE. The results of the sensitivity analysis and variance decomposition are shown in Figure 7 (black). Coefficient of variation (CV) is the uncertainty associated with each parameter, where the higher the CV the higher the uncertainty. Elasticity is the sensitivity of modeled LE to each parameter, where an elasticity of 1 indicates that model ouput will double when the parameter value doubles. The partial variance is the contribution of uncertainty from each parameter model output of LE as a function of both the parameter uncertainty and sensitivity.

For each of the parameters the sensitivity analysis showed that the parameters quantum efficiency and stomatal slope were the top parameters that the model output of LE was most sensitive to (Figure 7 Elasticity black). Cuticular conductance and leaf respiration rate had the highest uncertainty of all the tested parameters (Figure 7 CV (%) black). The combination of parameters uncertainty and sensitivity concluded that cuticular conductance, extinction coefficient of diffuse light, and stomatal slope in increasing order contribute the most uncertainty in model output of LE (Figure 7 Partial Variances black). In total, all the parameters contribute to 99% of the model output uncertainty which converts to over 27 W m^{-2}. Although quantum efficiency was one of the most sensitive parameters on model output of LE, it had the most confidence in the measurements as reported from BETYdb compared to the other parameters, therefore it does not contribute that much

uncertainty in the model results. From the results of the variance decomposition, the four parameters that contribute the most uncertainty to model LE of cuticular conductance, extinction coefficient of diffuse light, leaf respiration rate, and stomatal slope were chosen for further evaluation in PDA.

The goal of PDA is to update the estimates of the posterior distributions of the model parameters using observed data corresponded to model outputs. To update the prior distributions to be more optimal in terms of producing model output that matches observations, the batch method used employs the Markov Chain Monte Carlo (MCMC) techniques. This approach involves iteratively proposing a new set of model parameters, running the model with those parameters and comparing model output to the observed data (Dietze et al., 2012). When comparing model output to the observed values for LE, ustar (u^*) filtering was used. When u^* was greater than 0.4 m s^{-1} the observed values of LE for the same hour were ignored in this process. The MCMC algorithm generates random samples from the parameter distributions that can be used to approximate the full distribution. The algorithm then accepts or rejects the new parameters with some probability that depends upon the likelihood of generating the observed data under these parameters and the prior probability that those parameters are biologically realistic. This would result in narrower and more confident posterior distributions.

Now going back to the sensitivity analysis and variance decomposition but for the post-PDA results, cuticular conductance and leaf respiration rate decreased in uncertainty from the prior-PDA values (Figure 7 CV (%) blue). Those two parameters also increased in sensitivity while stomatal slope decreased in sensitivity as well as extinction coefficient for

diffuse light when compared to their pre-PDA values (Figure 7 Elasticity blue). The combination of the parameter uncertainty and sensitivity resulted with stomatal slope and extinction coefficient for diffuse light hardly adding any uncertainty to the model output of LE, less than 1% (Figure 7 Partial Variances blue). On the contrary, cuticular conductance and leaf respiration rate account for over 98% of the uncertainty in model output for LE. That converts to nearly 122 W m^{-2} which is greater than the 27 W m^{-2} for the pre-PDA uncertainty.

The post-PDA values for the selected parameters are as follows listed in Table 2 for the irrigated US-Ne2 and rain-fed US-Ne3. The distributions plotted in Figure 8 are for the prior distributions of the four selected parameters (green), post meta-analysis (black), post-PDA for US-Ne2 (blue) and US-Ne3 (red) with only stomatal slope having a post meta-analysis distribution. Extinction coefficient for diffuse light was the only parameter where the distribution became narrower and more confident. The other three parameters had their post-PDA distributions become wider than their prior distributions with US-Ne3 distributions slightly leaning more towards the lower values.

These results are inherently constrained by the current parameter distributions. Consequently, if the real values of the parameters are way outside of the prior ensemble confidence interval, data assimilation will not be able to fix this. When this happens, it could mean one of two things, 1) the prior parameter estimates must already be over-constrained, or 2) there are structural errors in the model itself that need fixing (“The Predictive Ecosystem Analyzer,” 2018).

Sensitivity analysis, uncertainty analysis, ensemble analysis, and PDA were used to understand the impacts of agricultural irrigation. To my knowledge this is the first study that

has used parameter data assimilation to further understand how the model handles the impacts of irrigation. The next section covers the observational analysis comparing US-Ne2 and US-Ne3 irrigational impacts on the environment as well as a more detailed look into the model output of LE from ensemble analysis, and pre- and post- PDA results.

4. Results

4.1 Observed impact of irrigation on LE

Irrigation that occurred was measured and recorded at site US-Ne2. Every year that corn was growing there was more measured precipitation at the irrigated site than the rain-fed site (Figure 9). There was approximately 284 (97%), 321 (56%), 266 (44%), 177 (18%), 59 (9%), and 113 (16%) mm more measured precipitation including irrigation at US-Ne2 (blue) than US-Ne3 (red) for the years 2001, 2003, 2005, 2007, 2009, and 2011 respectively. The difference in precipitation accumulation totals not occurring during the growing season between US-Ne2 (light blue) and US-Ne3 (light red) was 2, -18, 3, -5, -2, -10 mm where the negative values mean more precipitation was accumulated at US-Ne3 than US-Ne2. The growing season was defined as the 150-day period between planting (day of year 135) and harvest (day of year 285). These dates agreed with both sites as the planting date was the latest reported for all three sites for the years 2001 through 2007 and the harvest date was the earliest reported. The difference in growing season precipitation and irrigation accumulated totals between US-Ne2 (dark blue) and US-Ne3 (dark red) was 281 (80%), 339 (85%), 262 (85%), 182 (32%), 61 (14%), 124 (27%) mm greater at the irrigated US-Ne2 site for each year respectively. The annual total differences were driven by the irrigation accumulated at US-Ne2.

For each individual year the differences in precipitation become more pronounced when irrigation occurs during the growing season after the 150th day of the year (DOY) (Figure 10). The number of occurrences of irrigation were 10, 12, 12, 8, 6, and 6 times for the years 2001, 2003, 2005, 2007, 2009, and 2011 respectively. Not only were the irrigation counts less for the years 2007, 2009, and 2011, those growing season rainfall totals were all greater than 400 mm. The years 2001, 2003, and 2005 had more irrigational occurrences than the later years, and the growing season rainfall totals barely accumulated over 300 mm. For every year that corn was grown, there was a total of 54 individual irrigational occurrences that happened when rain was not occurring during the same time. The peak time of irrigation within the growing season occurred around July 20th (201st DOY) (Figure 11).

For the total of 54 irrigational occurrences, the differences in LE between the irrigated US-Ne2 and rain-fed US-Ne3 sites were calculated from the 24 hour averages of the day prior to irrigation and the three separate days after the occurrence (Figure 12 top left). Looking at the box and whisker plot, which shows the minimum as the lowest dash, first quartile as the region of the lowest line, second quartile as the bottom shaded region, third quartile as the top shaded region, fourth quartile as the highest line region, maximum as the upper most dash, mean as the 'X' mark, median as the middle line, and dots as the outlier points. The quartile calculations excluded the median. The negative values represent the variable was greater at the rain-fed US-Ne3 site and the positive values were where the variable was greater at the irrigated US-Ne2 site. The horizontal black line represented the median for the day prior to irrigation and the values in parentheses were the representative p-values for their respective time frames. A two-tailed distribution two sample of unequal

variances (heteroscedastic) t-test for $p > 0.05$ was performed with p-values rounded to the nearest thousandth. A p-value greater than 0.05 suggests there was no significant difference between the two sites.

Each day showed that there was a significant difference between the two sites with the p-value decreasing noticeably from 0.037 to 0.004 the day after irrigation. The difference between the two sites, although still significantly different, slightly increased in significance from the day immediately after irrigation to p-values of 0.005 and 0.011, two and three days post irrigation respectively. The median, which was approximately 20 W m^{-2} greater at the irrigated site the day prior to irrigation, increases slightly the day after irrigation, decreases the second day after irrigation, and increases again the third day after irrigation with the mean and medians for all the days were greater than zero, with only the lower quartiles reaching below zero.

It was important to look at the entire growing season of every year that corn was growing to see if this significant difference impacts the entire growing season than just the immediate days following the irrigational occurrences. Over the growing seasons, the LE at the irrigated site was approximately 12 W m^{-2} greater at the irrigated site (Table 3). This was a significant difference between the two sites. There were other significant irrigational impacts to the local meteorology than just LE.

4.2 Impact of irrigation on local meteorology

As stated in the previous section, irrigation impacted the partitioning of energy more towards LE at the irrigated site. The change in partitioning of energy has other implications for H, G, and RNET. With respect to H, all the days after irrigation showed a significant

difference between the two sites with the day prior, also being significantly different but with a slightly higher p-value than the other days at 0.001 (Figure 12 top right). The day prior to irrigation, the median was approximately 15 W m^{-2} greater at the rain-fed US-Ne3 site than irrigated US-Ne2. This increased to over 20 W m^{-2} greater at US-Ne3 the day following irrigation. This difference slowly decreased the following two and three days after irrigation. The first day after irrigation showed that every observation of H was greater at US-Ne3. The day prior, two, and three days after only had the upper quartile breaking past the zero mark. The entire growing season showed a significant difference of approximately 12 W m^{-2} between the two sites (Table 3).

As for G, there was not a significant difference between the two sites as p-values were all greater than 0.05 for every day (Figure 12 middle left). Every mean and median for each day was below zero, which represents more heating of the ground at the rain-fed US-Ne3 site than at the irrigated US-Ne2 site, while the top two quartiles stretched across zero. For the entire growing season, the average difference was not quite 1 W m^{-2} greater at US-Ne3 (Table 3). This was not a statistically significant difference as the p-value equaled 0.16.

Like G, RNET did not report any significant differences in the days surrounding irrigation (Figure 12 middle right). The day prior to irrigation reported a p-value of 0.324, this decreased to 0.081 after irrigation which was still not a significant difference between the two sites. The prior day median, which was not quite 10 W m^{-2}, and the following days were all greater at the irrigated US-Ne2 site, with the greatest increase between medians occurring between the day prior and day after irrigation occurred. The growing season average had RNET greater at US-Ne2 by over 8 W m^{-2}. On the contrary to the days

surrounding the irrigational event, this difference was a significant difference (p-value 0.001) (Table 3). The differences in RNET could partially be explained by the change in surface albedo which was not quantified in this thesis. As wet soils appear darker than dry soils, less radiation was then reflected away over the darker surface.

With the partitioning of RNET into LE, H, and G, the air temperature was 0.37 °C lower at US-Ne2 than at US-Ne3 site for the entire growing season (Table 3). This was not a statistically significant difference between the irrigated and rain-fed site (p-value 0.118). For the days around irrigation, there was no significant difference as p-values were 0.439, 0.222, 0.444, 0.548, for the day prior, day after, two days after, and three days after irrigation respectively (Figure 12 bottom left). One thing to note was the transition between prior and immediately after irrigation the temperature difference became more significant, but still not different enough to be statistically significant. The median for every day was near -0.5 °C with the day after irrigation being the coldest.

The soil temperature was a completely different story than the air temperature. Everyday around the time of irrigation was statistically significantly colder at the irrigated site (Figure 12 bottom right). There was a notable decrease in the temperature immediately following irrigation, that then slowly increased a few days after. The average and median for all the days were below zero along with the lowest three quartiles. As for the entire growing season, the soil was nearly 1°C colder at the irrigated US-Ne2 site than the rain-fed US-Ne3 site, which was a statistically significant difference (Table 3).

The RH was statistically significantly higher at the irrigated US-Ne2 site with the mean being over 5% greater than the rain-fed US-Ne3 site for the days surrounding the

irrigation (Figure 13 top left). The day immediately after irrigation all the observations were greater than zero. Over the entire growing season RH was also significantly greater the entire growing season at US-Ne2 by over 5% (Table 3).

Like RH, SWC was also significantly greater at US-Ne2 for the entire growing season by over 4% (Table 3). For the days around the irrigational occurrences, all reported significant differences between the two sites. All observations showed that SWC was greater at US-Ne2 than at US-Ne3 (Figure 13 top right), with the highest difference almost reaching 12% the day right after irrigation occurred. With more water being introduced to the surface, the increase in RH and SWC was as expected.

With the temperature being slightly lower and relative humidity being significantly higher at the irrigated than the rain-fed site, the VPD was significantly lower by over 1.5 hPa at the irrigated site for the growing seasons (Table 3). The significant difference was also noted for the days before and after irrigation (Figure 13 middle left). The greatest difference was also noted on the day occurring directly after irrigation with the maximum differences around 7 hPa.

As for GPP, the irrigated site reported over 1.5 μmol CO2 m^{-2} s^{-1} at the irrigated US-Ne2 site for the entire growing season which was a significantly different (Table 3). This difference varied with the timing of irrigation. The observed median and significant difference increased for each day with the third day after irrigation reporting the highest difference and the lowest p-value of 0.013 (Figure 13 bottom left).

Although not a significant difference, NEE also shows the average difference between the two sites increasing after irrigation with the third day reporting the greatest

difference (Figure 13 bottom right). This difference was noted for the growing seasons as the irrigated site reported nearly 1 μmol CO2 m^{-2} s^{-1} more than the rain-fed site, which was more significantly different (p-value 0.007) than the individual days surrounding the occurrence of irrigation (Table 3). This agreed with the statement that water stress free plants can be more productive.

4.3 Pre-PDA model BioCro response from irrigation

Looking at a 10-day period during the early part of the 2003 growing season in July with the first recorded irrigation occurring on July 4th (DOY 185) (Figure 14 top). This figure shows the observed latent heating at US-Ne2 (solid black) and US-Ne3 (dashed black) compared with the pre-PDA model ensemble mean in blue (US-Ne2) and red (US-Ne3) and 2.5 to 97.5% confidence interval in their respective color shaded fill with the observed rainfall (red bar) and irrigation + rainfall (blue bar). Before the irrigation occurred, both sites underestimated LE. After the irrigation, LE was shown to be greater at US-Ne2, but still not as great as the observed value. After the reported rain just two days after the irrigation, the LE values increased at US-Ne3 to be near US-Ne2 values. This then decreases the next day with the LE being greater at US-Ne2. The observed LE generally increased through this entire period from over 300 W m^{-2} at the beginning to over 400 W m^{-2} by the end. The model results fluctuated between under to over 300 W m^{-2}.

The middle of the growing season that closely follows the peak of irrigational occurrences over the 10-day period from July 29th (DOY 210) up to August 8th (DOY 220) as this period shows two instances of irrigation on DOY 212 and DOY 216 (Figure 14 middle). The differences in the daily maximums of LE between the irrigated US-Ne2 and rain-fed US-

Ne3 site were shown in both the observations and model results. The maximum magnitudes were not as well reciprocated as the observed values reach maximums well over 400 W m^{-2} with the model results hardly ever breaking over 400 W m^{-2}.

In the later part of the growing season of September 3rd (DOY 246) to September 13th (DOY 256), the last observed occurrence of irrigation was on DOY 247 (Figure 14 bottom). The observed LE for US-Ne2 reached daily maximums near 400 W m^{-2} where US-Ne3 observed LE never broke over 200 W m^{-2}. For the model results, the confidence intervals were wider than the mid and early season confidence intervals. Contradicting the observations, the model had the rain-fed US-Ne3 site on average greater than the irrigated site. The day after the three-day rainy period (DOY 252 to DOY 255), the observed LE at the irrigated site increased back to its previous values of a daily maximum near 400 W m^{-2}. To partially explain this response and as stated previously, the observed SWC at US-Ne2 showed that it was significantly greater than at US-Ne3.

The low bias in model results of LE at both sites during the rainy periods could partially be explained from the fact that the instruments measuring LE were sensitive under cloudy conditions. This would throw off the observational results from the truth. In general, the early- and mid-season model results underestimated LE for both sites. The late season model results overestimated LE at US-Ne3 and underestimated LE for US-Ne2.

4.4 Post-PDA model BioCro response from irrigation

Looking at the same 10-day periods throughout the growing season mention previously, the post-PDA model results showed a widening of the confidence intervals from the previous pre-PDA results (Figure 15). For the early- and mid-season periods, LE was

underestimated for both sites with the rain-fed US-Ne3 site showing more of an underestimation than previous results. The highest value within the confidence interval for the irrigated US-Ne2 site were closer to the true observed values.

The later part of the season was better captured post-PDA. The maximum values within the confidence interval for US-Ne2 site were nearly a match of the observed values for that irrigated site. The ensemble mean for US-Ne3 was also a near match for the observed values at that rain-fed site.

The differences in the ensemble mean for both sites were as follows in Figure 16 with the same observations at each site and the lines now represent the pre-PDA ensemble mean minus the post-PDA ensemble mean for each site in their respective colors of blue for the irrigated US-Ne2 site and red for the rain-fed US-Ne3 site. Positive values represent greater values in LE pre-PDA and negative values represent greater values in LE post-PDA. For the early season period, there was a reduction of the average LE values in the later part of each diurnal cycle from pre- to post-PDA. The mid-season showed an even larger decrease from pre-PDA to post-PDA in LE at US-Ne3 and only a slight decrease at US-Ne2. The more extreme changes occurred during the latter part of the growing season. The LE mean values increased at US-Ne2 near the middle of each day with a decrease in the near ending of each day. US-Ne3 showed a decrease in the ensemble mean of LE from pre-PDA to post-PDA to follow more closely with the observed values.

4.5 Model error

It was important to look at the whole year as well as the previously analyzed shorter time frames. Model error was the difference between the ensemble mean and the observed

LE. There was some variability between under and overestimating LE before the growing season, early into the growing season, and late growing season past harvest in both ensemble runs pre- and post-PDA (Figure 17). For both sites during the main part of the growing season, LE values were underestimated both pre- and post-PDA. Although for US-Ne3, there was less overestimation from the mid growing season to late growing season post-PDA.

Theses hourly errors accumulated during the whole year were shown in Figure 18 for pre-PDA (top) and post-PDA (bottom) for the year 2003 at US-Ne2 (blue) and US-Ne3 (red) with the 2.5 to 97.5% confidence interval in the respective sites shaded color where the black line represents no error between model and observations. Pre-PDA results show that both sites underestimated LE slightly for the beginning of the growing season. The transition between early and mid-season the model results leveled out for a short period then began to underestimate for the middle of the growing season. US-Ne3 then began to start overestimating LE for the late growing season before leveling off post-harvest. The year-end model error accumulation for US-Ne3 was approximately over by a total of 24,130 W m^{-2}. On the other hand, US-Ne2 underestimated LE values for the rest of the growing season before leveling off after harvest with a total underestimated value near 79,451 W m^{-2}. Even the maximum values within the confidence interval had underestimated values of LE at US-Ne2 for the later part of the growing season.

Although the confidence interval did expand from pre-PDA to post-PDA, post-PDA model results showed that both sites stayed closer to the no error line further into the growing season. This trend did not continue as both US-Ne2 and US-Ne3 underestimated LE during the mid-growing season. US-Ne3 did level off for the later growing season which was an

improvement to the overestimation noted at this time for the pre-PDA model run. US-Ne3 total underestimation came out to 72,867 W m^{-2}. As for US-Ne2, there was underestimation of LE like the pre-PDA model results, but the total underestimation was even more at 103,696 W m^{-2}. The maximum values within the confidence interval did overlap the no error line, which was an improvement from the pre-PDA ensemble run.

5. Discussion

5.1 Questions raised

Does BioCro capture the effect of irrigation on LE? This first posed question can be answered simply as no. The pre-PDA model results did however capture the diurnal cycle of LE well enough, but it underestimated how quickly it would taper off later in the day. The average ensemble magnitudes were underestimated at both sites for most of the growing season with the irrigated US-Ne2 site showing more underestimated values in the later part of the growing season before harvest. The growing season hourly mean difference between the two sites was greater at US-Ne3 by over 3.5 W m^{-2}.

Was the model improved with observations? By using observations, PDA did slightly replicate the effects of irrigation on LE. The growing season hourly mean difference between the two sites was greater at US-Ne2 by over 13 W m^{-2}. Although this value was closer to the observed mean difference, the individual sites magnitudes were slightly improved. These improvements were seen at US-Ne3 where there were overestimated pre-PDA values of LE in the later part of the growing season that were not as overestimated post-PDA. During the main part of the growing season there was still underestimation of LE. For US-Ne2, LE was still underestimated for the growing season, but it was less underestimated near the ending of

the growing season. This reveals that the model parameters can only partially improve the model results. Although model improvement was not the focus of this thesis work, it brings more attention to understanding the system and what affects LE. One direction to further investigate is how phenology was represented as the above-mentioned improvements were noted for different parts of the growing season.

Knowing that the observational uncertainty adds uncertainty to model output, model sensitivity to temperature was evaluated. For a single run during the year 2003 where neither temperature nor any parameters were changed, growing season LE was higher at the rain-fed site by 3.8%. Hourly temperatures were changed by ±1 and ±2 degree(s) Celsius for four separate model runs to compare to the original model run with the actual observed temperature. For the tests of +1, +2, -1, and -2°C, the LE was greater at the rain-fed site by 5.1%, 6.2%, 4.1%, and 2.2% respectively. These results did not show any significant change nor improvement. This agreed with Dietze (2017) that similar to NEE the model results of LE were not as sensitive to the initial conditions as the model plant parameters.

5.2 Mechanisms of enhanced ET with irrigation

One major part of calculating LE, was knowing how much energy transpiration and evaporation were contributing to the total value of LE. There are multiple ways that irrigation impacts transpiration and evaporation. As previously mentioned, plants that are water-stress free can grow and produce more, which results in more transpiration. Observations for the years 2001, 2003, and 2005 at these sites confirm this as the maximum LAI, maximum height, and grain yield were all greater at the irrigated US-Ne2 site (Table 4).

Regarding an increase in LAI from irrigated to non-irrigated crops, the model pre-PDA ensemble mean for 2003 of maximum LAI were 13.04 with a 2.5 to 97.5% confidence interval from 7.69 to 16.16 for US-Ne2 and 12.23 with a 2.5 to 97.5% confidence interval from 6.86 to 16.34 for US-Ne3. This shows that the model did capture the effect of irrigation on maximum LAI, but these values were all greater than the observations. The confidence interval was narrower for US-Ne2, showing that there was more uncertainty at the rain-fed US-Ne3 when modeling LAI. An increase of LAI results in more intercepted light and rainfall that does not reach the ground. This would lower soil evaporation, making transpiration during the growing season the dominant contributor to LE.

Figure 19 shows the pre-PDA model ensemble of transpiration and evaporation contributions to total LE compared to the observations of LE for each site for the year 2003. At both sites, soil evaporation dominates early in the year, but during the growing season it was transpiration that was the main contributor. As stated previously, the later part of the growing season was where values of LE were overestimated. This was due to transpiration, hinting that the model plant phenology stage still represented ‘green’ crops that were not yet in the senescence stage. This further emphasizes the importance of correctly modeling phenology stages.

5.3 Comparison to other studies

Previous studies have looked at irrigation over large expansive areas, the advantage of this point model simulation was that the two sites were close to one another and experienced approximately the same climatic conditions that would otherwise decrease in correlation with increasing spatial distance. To my knowledge, this is the first study to utilize

PDA to improve model results for latent heating when irrigation was occurring. Other studies have looked at irrigational effects using several different models, this is the first study done using the model BioCro for sensitivity analysis.

The observations from the irrigated site US-Ne2 and rain-fed site US-Ne3 agree with previous studies on the observational effects of irrigation. The observed decrease in temperature from rain-fed to irrigation was not quite 0.1 °C for the growing season. The decreasing trend agrees with previous studies, but the magnitude of the decrease was relatively small compared to the other studies. Adegoke et al., (2003) showed that the average near ground air temperature was 1.2°C less over Nebraska due to irrigation and a maximum cooling of almost 3.5°C for the two-week time frame. They used satellite derived estimate of irrigated farmland acreage in Nebraska as the control run with the RAMS model fine grid spacing of 10 km. They compared the irrigational control run to the RAMS model using the Olson Global Ecosystem (OGE) dry vegetation dataset. The differences in temperature magnitude could be from the defined area of satellite derived irrigation as in this thesis study that the sites were within 1.6 km of each other. The differences in temporal averaging could also explain some of the differences in magnitude as the authors averaged the entire inner spatial domain over a couple weeks and not the entire growing season.

On the moisture side of this comparison, Barnston and Schickedanz (1984) had the RH as a 25% increase from the dry to irrigated scenarios. This was larger than the 5% increase in RH from the rain-fed US-Ne3 to irrigated US-Ne2. For their study, their domain was over the southern U.S. great plains focused on the Texas panhandle. The western side of Texas is climatically dry, with a dry line being very prominent during the summer. The

variation and propagation of that dry line in combination with irrigation in the panhandle could explain the large magnitude difference between the dry and irrigated tests.

A model data comparison study of carbon and energy fluxes in cropland ecosystems by Lokupitiya et al. (2016) compared 20 different models with the observations of net ecosystem exchange, latent, and sensible heat at five different eddy covariance flux tower sites within the Midwest agricultural plains. These sites included US-Ne1, US-Ne2, US-Ne3, US-IB1, US-ARM. Out of the 20 models, only five were agricultural models which included Agro-IBIS, DNDC, EPIC, ORCHIDEE-STICS, and SiBcrop. In conclusion, the authors found that most of the models had higher H, lower LE, and lower NEE compared to the observations. Between the Mead, NE irrigated and rain-fed sites regarding maize, the overall model mean of NEE had higher skills at the irrigated sites and poorer model performance at the rain-fed site. Models that had crop specificity accurately simulated the magnitude of carbon flux. Like NEE, model performance of LE was better at irrigated sites than the rain-fed site for maize. For H, there was not much difference in skill between the irrigated and rain-fed sites with an overall poor model performance. They also reported that there was no difference in model performances based on the model formulation for photosynthesis or on diagnostic versus prognostic phenology. Crop-specific parameterizations within the models could help better simulation of the inter-annual variability of fluxes under crop rotation (Lokupitiya et al., 2016).

Suyker et al. (2004) studied the effects of irrigation on NEE at the same Mead, NE eddy covariance flux towers used in this study. For the first year of this study in 2001, they concluded that NEE was reduced under moisture stress. Nighttime NEE was exponentially

related to soil temperature when not under moisture stress, while daytime NEE was smaller at the rain-fed site. This could be from lower green LAI, which likely resulted from a lower planting density at that site, different planting dates, and the effect of moisture stress. Peaks in GPP were observed approximately the same time as the occurrence of maximum LAI. Overall, the eddy covariance measurements of CO2 really helped them monitor the net gain of carbon during the growing season reasonably well.

Since this thesis work focused on latent heating increase between two sites that were close to one another, the point source model run could initially capture some of the differences in LE. Once the model was run with the post-PDA calibrated parameters, the model could pick up on the daily differences in latent heating better, but the growing season values were still underestimated even with the differences between the sites became more prominent. The differences between different model's spatial scale can partially explain the variance between the other studies. Overall these results are consistent with previous findings, but there were some differences in magnitude between the model results and observations of the irrigational effect on temperature, LE, LAI, and other atmospheric variables.

5.4 Uncertainty and paths forwards

Following what other studies have done and the results covered in this project bring to light a few areas that can improved, with the first area being our understanding of plant parameters. The model was sensitive to cuticular conductance, extinction coefficient for diffuse light, leaf respiration rate, and stomatal slope. After PDA the model was sensitive to cuticular conductance and leaf respiration rate. There were a combined 33 observations of

these variables with 32 representing leaf respiration rate and the other one for stomatal slope. This emphasizes the need for more observations to be made, especially for cuticular conductance as the measurements were lacking, and the model output of LE was extremely sensitive to the parameter.

More work should also be done on the model structure and how it processes these parameters. One test could be done to compare different transpiration methods. These could include the Penman-Monteith, Penman-potential, and Priestley-Taylor models for transpiration. The Penman-potential transpiration model has been shown to overestimate transpiration in the model BioCro (Miguez, 2015). I would expect that the Penman-potential method to represent the transpiration of irrigated corn in the Mid-West U.S. as corn is a highly transpiring crop. To handle the phenology stage issue, there is a maize model currently under development. The model was run with the parameters suited for maize, but it was run under the general biomass growing function.

Uncertainties in surface temperatures due to irrigational cooling implies larger uncertainties for future climate predictions. It is important to consider these irrigational effects under future climate scenarios. Even though the model did not show much change in LE for the temperature tests, that does not mean the LE will not change in the future. As I tested the model on its temperature sensitivity, I did not want to replicate future global scenarios. Under future climate prediction changes besides temperature increases, there are other likely changes to CO2 concentration, precipitation patterns, and the economy. Each of these changes has future implications of irrigation and its impacts. It would be unwise to model, as irrigation is controlled by the farmers. Since models cannot fully compute all the

processes from the tiniest plant cells to ENSO events under current computing standards, it is impossible for the current models with limited computing power to handle how the human brain processes facts to make decisions.

It should be noted that there are several other farm management practices besides irrigation that can impact the water, carbon, and energy cycles. These include but are not limited to tillage practice, pesticide/fertilizer application timing and frequency, irrigation type (drip, central pivot, sprinkler, sub-irrigation, flood, etc.), and crop type. To expand on this study, the soybean growing years should be analyzed. The differences in the practices can also explain differences in observations of LE and irrigational impacts variation between the different studies. Future work could be exploring these other impacts on latent heating, for example by including the nitrogen parameterizations for the model runs.

Future work will include additional observational analysis of maximum and minimum temperature impacts from irrigation and post-PDA ensemble analysis of evapotranspiration and LAI. The model results will be verified by comparing the observed NEE and GPP to the modeled NPP. The work done further emphasizes how close and how far away models are at capturing this effect of irrigation on latent heating which adds motivation for future work to be done in order to further understand the dynamics of the system.

6. Conclusion

With an increasing global population, agricultural intensification and expansion further signifies the importance of understanding what the impacts of irrigation practices could mean for the atmosphere. In conclusion, the year 2003 showed the greatest differences in LE between the irrigated and rain-fed sites. This was because there was a relatively dry

period during the growing season when the crops were most productive. There were regularly timed irrigational occurrences approximately every 4 days between applications. Days after irrigation, LE was greater at the irrigated site. These lasting effects can partially be due to the increased soil moisture. Other significant impacts of irrigation include H, RNET, TS, RH, SWC, VPD, GPP, and NEE for the growing season. With a focus on LE, model results did not capture the resulting effects from irrigation well. These results were slightly improved with the observations through PDA, with most of the change occurring in the later part of the growing season. This agrees with previous studies that the phenology stage of the crop greatly impacts the rate of evapotranspiration and resulting carbon and energy cycles.

Many farmers are more concerned with maximizing profits and not necessarily increasing yields. While irrigation does increase yields, it does not mean that it is always cost effective. In the end, it comes down to what the farmer decides. From their decisions, the resulting complex feedbacks from the agricultural practices impact yield and land-atmosphere interactions. To improve our understanding of the system and what changes to the system could impact, further work must include more measurements of plant parameters to reduce uncertainty of the model results, further investigation on soil moisture and canopy interception of rainfall, research of the crop phenology representation by the model, and further validation of the model by investigating LAI and NPP to further understand how the system was represented by the model.

The purpose of this study was to understand the impact that farmers' decisions to irrigate have on the local climate and to understand how the system was impacted by that decision. It was made clear that there was a noticeable impact on the system affecting the

water, carbon, and energy cycles. There is no reason that this work should stop. Further investigation is needed in order to fully understand how the land and atmosphere interact with the alteration to that system through irrigation as it impacts all of our lives one way or another.

References

Adegoke, J. O., Pielke Sr., R. A., Eastman, J. Mahmood, R., & Hubbard, K. J. (2003). Impact of irrigation on midsummer surface fluxes and temperature under dry synoptic conditions: a regional atmospheric model study of the U.S. High Plains. *Monthly Weather Review, 131,* 556-564.

Alter, R. E., Im, E., & Eltahir, E. A. (2015). Rainfall consistently enhanced around the Gezira Scheme in East Africa due to irrigation. *Nature Geoscience, 8*(10), 763-767. doi:10.1038/ngeo2514

Bagley, J. E., Desai, A. R., Dirmeyer, P. A., & Foley, J. A. (2012). Effects of land cover change on moisture availability and potential crop yield in the world's breadbaskets. *Environmental Research Letters, 7*. doi:10.1088/1748-9326/7/1/014009

Bagley, J. E., Davis, S. C., Georgescu, M., Hussain, M. Z., Miller, J., Nesbitt, S. W., … Bernacchi, C. J. (2014). The biophysical link between climate, water, and vegetation in bioenergy agro-ecosystems. *Journal of Biomass and Bioenergy, 71,* 187-201. doi:10.1016/j.boimboie.2014.10.007

Baldocchi, D. D., Hicks, B. B., & Meyers, T. P. (1988). Measuring biosphere-atmosphere exchanges of biologically related gasses with micrometeorological methods. *Ecology 69*(5), 1331-1340.

Ball, J.T., Woodrow, I.E., & Berry, J.A. (1987). A model predicting stomatal conductance and its contribution to the control of photosynthesis under different environmental conditions. In: Biggins J. (Ed.) *Progress in photosynthesis research* (pp. 221-224). Dordrecht, Netherlands: Springer

Barnston, A. G., & Schickedanz, P. T. (1984). The effect of irrigation on warm season precipitation in the Southern Great Plains. *Journal of Climate and Applied Meteorology,* 23(6), 865-888.

Bonfils, C., & Lobell, D. (2007). Empirical evidence for a recent slowdown in irrigation-induced cooling. *Proceedings of the National Academy of Sciences, 104*(34), 13582-13587. doi:10.1073/pnas.0700144104

Bright, R. M., Davin, E., O'Halloran, T., Pongratz, J., Khao, K., & Cescatti, A. (2017). Local temperature response to land cover and management change driven by non-radiative processes. *Nature Climate Change, 7*(4), 296-302. doi:10.1038/nclimate3250

Campbell, G. S., & Norman, J. M. (1998). *An introduction to environmental biophysics.* New York, NY: Springer-Verlag

Collatz, G. J., Ribas-Carbo, M., & Berry, J. A. (1992). Coupled photosynthesis-stomatal conductance model for leaves of c4 plants. Australian Journal of Plant Physiology, 19(5), 519-538.

Dale, V. H., Kline, K. L., Wiens, J., & Fargione, J. (2010). Biofuels: implications for land use and biodiversity. *Ecological Society of America*. Retrieved from http://www.esa.org/biofuelsreports/files/ESA%20Biofuels%20Report_VH%20Dale%20et%20al.pdf

DeAngelis, A., Dominguez, F., Fan, Y., Robock, A., Kustu, M. D., & Robinson, D. (2010). Evidence of enhanced precipitation due to irrigation of the Great Plains of the United States. *Journal of Geophysical Research, 115*. doi:10.1029/2010jd013892

Decker, M., Ma, S., & Pitman, A. (2017). Local land – atmosphere feedbacks limit irrigation demand. *Environmental Research Letters, 12*. doi:10.1088/1748-9326/aa65a6

Dietze, M. C., LeBauer, D. S., & Kooper, R. (2012). On improving the communication between models and data. *Plant, Cell, & Environment, 36*(9), 1575-1585. doi:10.1111/pce.12043

Dietze, M. C. (2017). Prediction in ecology: A first-principles framework. *Ecological Applications, 27*(7), 2048-2060.

Deryng, D., Sacks, W. J., Barford, C. C., & Ramankutty, N. (2011). Simulating the effects of climate and agricultural management practices on global crop yield. *Global Biogeochemical Cycles, 25*, GB2006. doi:10.1029/2009GB003765

Douglas, E. M., Niyogi, D., Frolking, S., Yeluripati, J. B., Pielke Sr., R. A., Niyogi, N., … Mohanty, U. C. (2006) Changes in moisture and energy fluxes due to agricultural land use and irrigation in the Indian Monsoon Belt. *Geophysical Research Letters, 33*, L14403. doi:10.1029/2006GL026550

Douglas, E. M., Beltran-Przekurat, A., Niyogi, D., Pielke Sr., R. A., Vorosmarty, C. J. (2009). The impact of agricultural intensification and irrigation on land-atmosphere interactions and Indian monsoon precipitation – a mesoscale modeling perspective. *Global and Planetary Change, 67*, 117-128. doi:10.1016/j.gloplacha.2008.12.007

Eltahir, E. A. B. (1998) A soil moisture-rainfall feedback mechanism 1. Theory and observations. *Water Resources Research, 34*(4), 765-776.

Farmer, B. H. (1986). Perspectives on the ‘Green Revolution’ in South Asia. *Modern Asian Studies, 20*(1), 175-199.

Farquhar, G. D., von Caemmerer, S., & Berry, J. A. (1980). A biochemical model of photosynthetic CO2 assimilation in leaves of C3 species. *Planta, 149*, 78-90.

Foken, T. (2008). The energy balance closure problem: An overview. *Ecological Applications, 18*(6), 1351-1367.

Hatch, M. D., & Slack, C. R. (1968). A new enzyme for the interconversion of pyruvate and phosphopyruvate and its role in the C4 dicarboxylic acid pathway of photosynthesis. *Biochemical Journal, 103*(3), 660-665. doi:10.1042/bj1030660

Harding, K. J., & Snyder, P. K. (2012). Modeling the atmospheric response to irrigation in the Great Plains. Part I: General impacts on precipitation and the energy budget. *Journal of Hydrometeorology, 13*(6), 1667-1686. doi:10.1175/jhm-d-098.1

Humphries, S. W., & Long, S. P. (1995). WIMOVAC: A software package for modelling the dynamics of plant leaf and canopy photosynthesis. *Bioinformatics, 11*(4), 361-371. doi:10.1093/bioinformatics/11.4.361

Im, E., Marcella, M. P., & Eltahir E. A. B., (2013). Impact of potential large-scaled irrigation on the West African Monsoon and its dependence on location of irrigated area. *Journal of Climate, 27*(3), 994-1009. doi:10.1175/jcli-d-13-00290.1

Jacobs, A. F., Heusinkveld, B. G., & Holtslag, A. A. (2008). Towards closing the surface energy budget of a mid-latitude grassland. *Boundary-Layer Meteorology, 126*(1), 125-136. doi:10.1007/s10546-007-9209-2

Jones, H. G., & Rotenberg, E. (2011). Energy, radiation and temperature regulation in plants. *Encyclopedia of Life Sciences*. John Wiley & Sons Ltd, Chichester. doi:10.1002/9780470015902.a0003199.pub2

Kucharik, C. J. (2003). Evaluation of a process-based agro-ecosystem model (Agro-IBIS) across the U.S. Corn Belt: Simulations of the interannual variability in maize yield. *Earth Interactions, 7*(14).

Kucharik, C. J., & Twine, T. E. (2007). Residue, respiration, and residuals: Evaluation of a dynamic agroecosystem model using eddy flux measurements and biometric data. *Agricultural and Forest Meteorology, 146,* 134-158. doi:10.1016/j.agrformet.2007.05.011

Leakey, A. D. B., M. Uribelarrea, E. A. Ainsworth, S. L. Naidu, A. Rogers, D. R. Ort, & S. P. Long. (2006). Photosynthesis, productivity, and yield of maize are not affected by open-air elevation of CO2 concentration in the absence of drought. *Plant Physiology, 140*(2), 779-790. doi:10.1104/pp.105.073957

LeBauer, D. D., Dietze, M., Kooper, R., Long, S., Mulrooney, P., Rohde, G. S., & Wang, D. (2010). Biofuel Ecophysical Traits and Yields database (BETYdb). Energy Biosciences Institute, University of Illinois at Urbana-Champaign. doi:10.13012/J8H41PB9

LeBauer, D. S., Wang, D., Richter, K. T., Davidson, C. C., & Dietze, M. C. (2013). Facilitating feedbacks between field Measurements and ecosystem models. *Ecological Monographs, 83*(2), 133-154.

Lokupitiya, E., Denning, S., Paustian, K., Baker, I., & Schaefer, K. (2009). Incorporation of crop phenology in Simple Biosphere Model (SiBcrop) to improve land-atmosphere carbon exchanges from croplands. *Biogeosciences, 6,* 969-986.

Lokupitiya, E., Denning, A. S., Schaefer, K., Ricciuto, D., Anderson, R., Arain, M. A., … & Xue, Y. (2016). Carbon and energy fluxes in cropland ecosystems: A model data comparison. *Biogeochemistry, 129,* 53-76. doi:10.1007/s10533-016-0219-3

Lu, Y., Harding, K., & Kueppers, L. (2017). Irrigation effects on land-atmosphere coupling strength in the United States. *Journal of Climate, 30,* 3671-3685. doi:10.1175/JCLI-D-15-0706.1

McMahon, S. M., Dietze, M. C., Hersh, M. H., Moran, E. V., & Clark, J. S. (2009). A predictive framework to understand forest responses to global change. *The Year in Ecology and Conservation Biology, 1162,* 221-236. doi:10.1111/j.1749-6632.2009.04495.x

Miguez, F. E., Zhu, X., Humphries, S., Bollero, G. A., & Long, S. P. (2009). A semimechanistic model predicting the growth and production of the bioenergy crop Miscanthus×giganteus: Description, parameterization and validation. *Global Change Biology Bioenergy, 1*(4), 282-296. doi:10.1111/j.1757-1707.2009.01019.x

Miguez, F. E. (2015). Simulation and parameter estimation for biomass crops. Retrieved from http://biocro.r-forge.r-project.org/

Nobel, P. S. (1974). *Introduction to biophysical plant physiology*. San Francisco, CA: Freeman.

Ozdogan, M., & Gutman, G. (2008). A new methodology to map irrigated areas using multi-temporal MODIS and ancillary data: An application example in the continental US. *Remote Sensing of Environment, 112,* 3520-3537. doi:10.1016/j.rse.2008.04.010

The Predictive Ecosystem Analyzer. (2018). GitHub Pages. https://pecanproject.github.io/pecan-documentation/master/index.html#

Pielke Sr, R. A., Marland, G., Betts, R. A., Chase, T. N., Eastman, J. L., Niles, J. O., … Running, S. W. (2002). The influence of land-use change and landscape dynamics on the climate system: relevance to climate-change policy beyond the radiative effect of greenhouse gasses. *Philosophical Transaction of the Royal Society A, 360,* 1705-1719. doi:10.1098/rsta.2002.1027

Reichstein, M., Falge, E., Baldocchi, D., Papale, D., Aubinet, M., Berbigier, P., … Valentini, R. (2005). On the separation of net ecosystem exchange into assimilation and ecosystem respiration: review and improved algorithm. *Global Change Biology, 11,* 1424-1439. doi:10.1111/j.1365-2486.2005.001002.x

Rosegrant, M. W., Cai, X., & Cline, S. A. (2002). World water and food to 2025. Washington, DC: International Food Policy Research Institute (IFPRI).

Siebert, S., & Doll, P. (2010). Quantifying blue and green virtual water contents in global crop production as well as potential production losses without irrigation. *Journal of Hydrology, 384,* 198-217. doi:10.1016/j.jhydrol.2009.07.031

Snyder, R. L., & Melo-Abreu, J. P. (2005). Frost protection: fundamentals, practice and economics. Rome: Food and Agriculture Organization of the United Nations

Srivastava, L. M., & Singh, A. P. (1972) Stomatal structure in corn leaves. *Journal of Ultrastructure Research,* 39, 345-363.

Suyker, A. E., Verma, S. B., Burba, G. G., Arkebauer, T. J., Walters, D. T., & Hubbard, K. G. (2004). Growing season carbon dioxide exchange in irrigated and rainfed maize. *Agriculture and Forest Meteorology, 124,* 1-13. doi:10.1016/j.agrformet.2004.01.011

Verma, S. B., Dobermann, A., Cassman, K. G., Walters, D. T., Knops, J. M., Arkebauer, T. J., … Walter-Shae, E. A. (2005). Annual carbon dioxide exchange in irrigated and rainfed maize-based agroecosystems. *Agricultural and Forest Meteorology, 131,* 77-96. doi:10.1016/j.agrformet.2005.05.003

United Nations, Department of Economic and Social Affairs, Population Division. (2017). World Population Prospects: The Revision, Data Booklet. ST/ESA/SER.A/401

United States Department of Agriculture, National Agriculture Statistics Service. (2014). 2012 Census of agriculture. Special Studies: Part 1. Farm and ranch irrigation survey (2013) Volume 3 AC-12-SS-1

United States Department of the Interior, U.S. Geological Survey. (2016). Evapotranspiration – the water cycle. Retrieved from https://water.usgs.gov/edu/watercycleevapotranspiration.html

Wright, I. J., Reich, P. B., Westoby, M., Ackerly, D. D., Baruch, Z., Bongers, F., … Villar, R. (2004). The worldwide leaf economics spectrum. *Nature, 428,* 821-827. doi:10.1038/nature02403

Wullschleger, S. D. (1993). Biochemical limitations to carbon assimilation in C3 plants: A retrospective analysis of the A/Ci curves from 109 species. *Journal of Experimental Botany, 44*(5), 907-920. doi:10.1093/jxb/44.5.907

Yamori, W., Hikosaka, K., & Way, D. A. (2014). Temperature response of photosynthesis in C3, C4, and CAM plants: temperature acclimation and temperature adaptation. *Photosynthesis Research, 119*(1), 101-117. doi:10.1007/s11120-013-9874-6

Figures

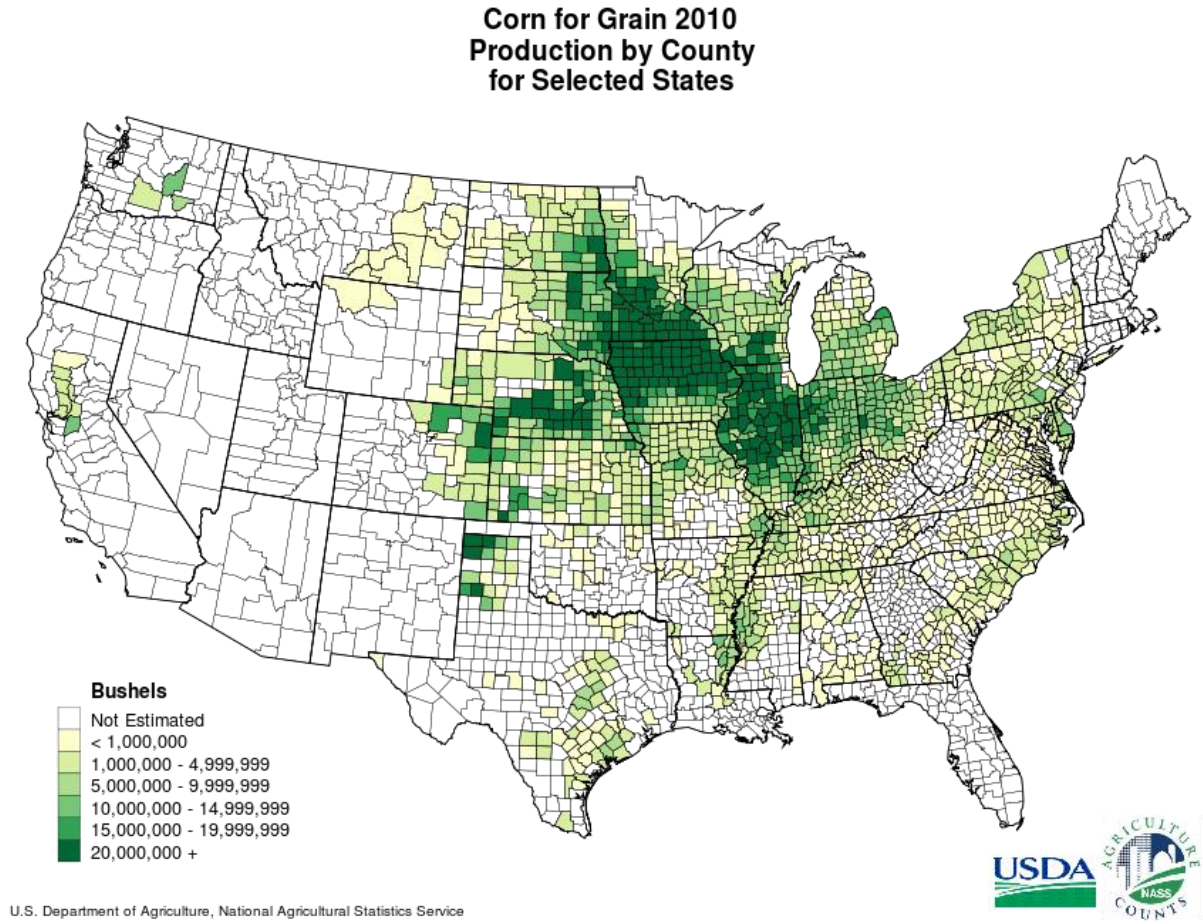

Figure 1: Corn production for grain in bushels (USDA).

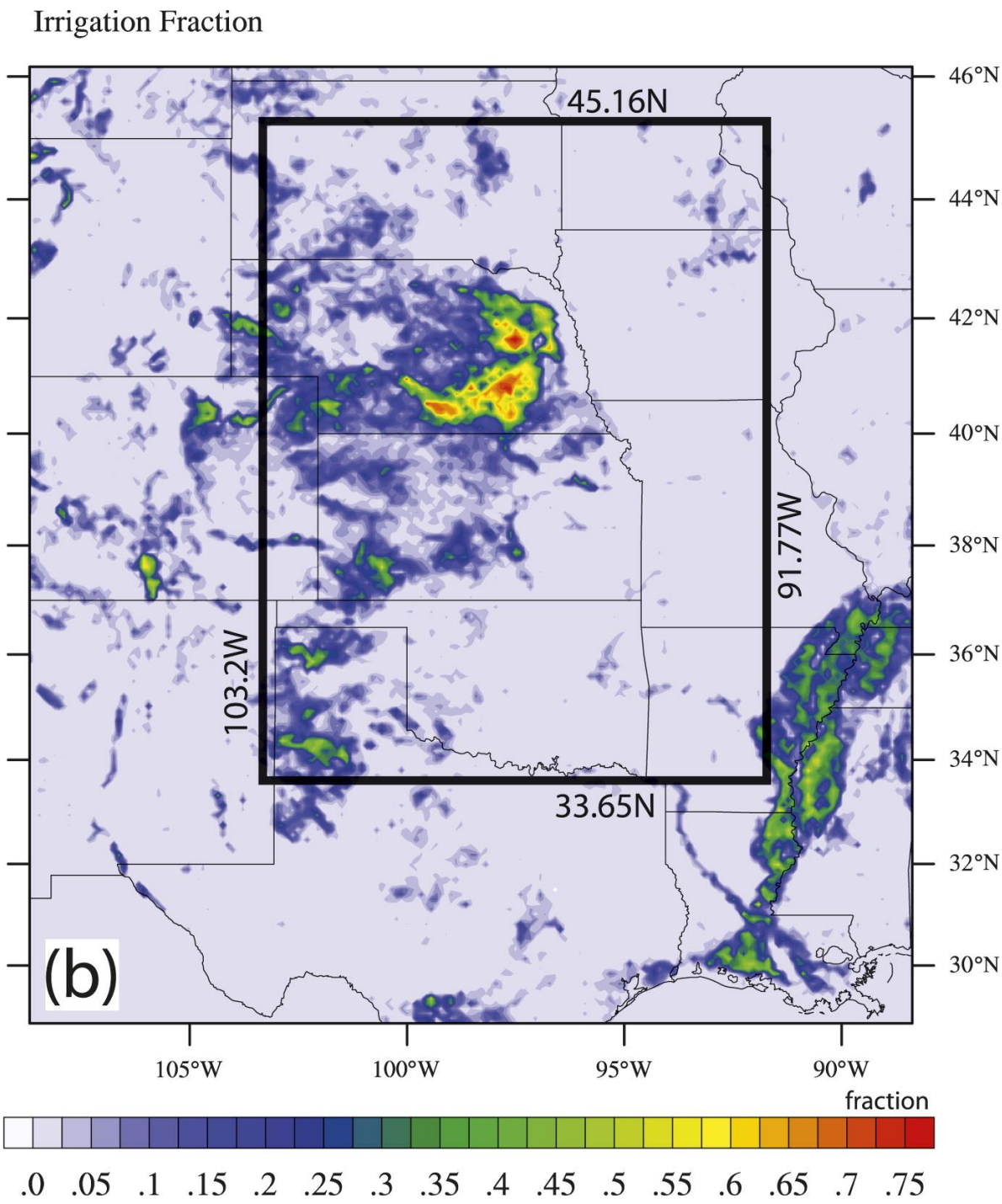

Figure 2: Irrigated fraction from Ozdogan and Gutman (2008) over the WRF domain (Harding & Snyder, 2012)

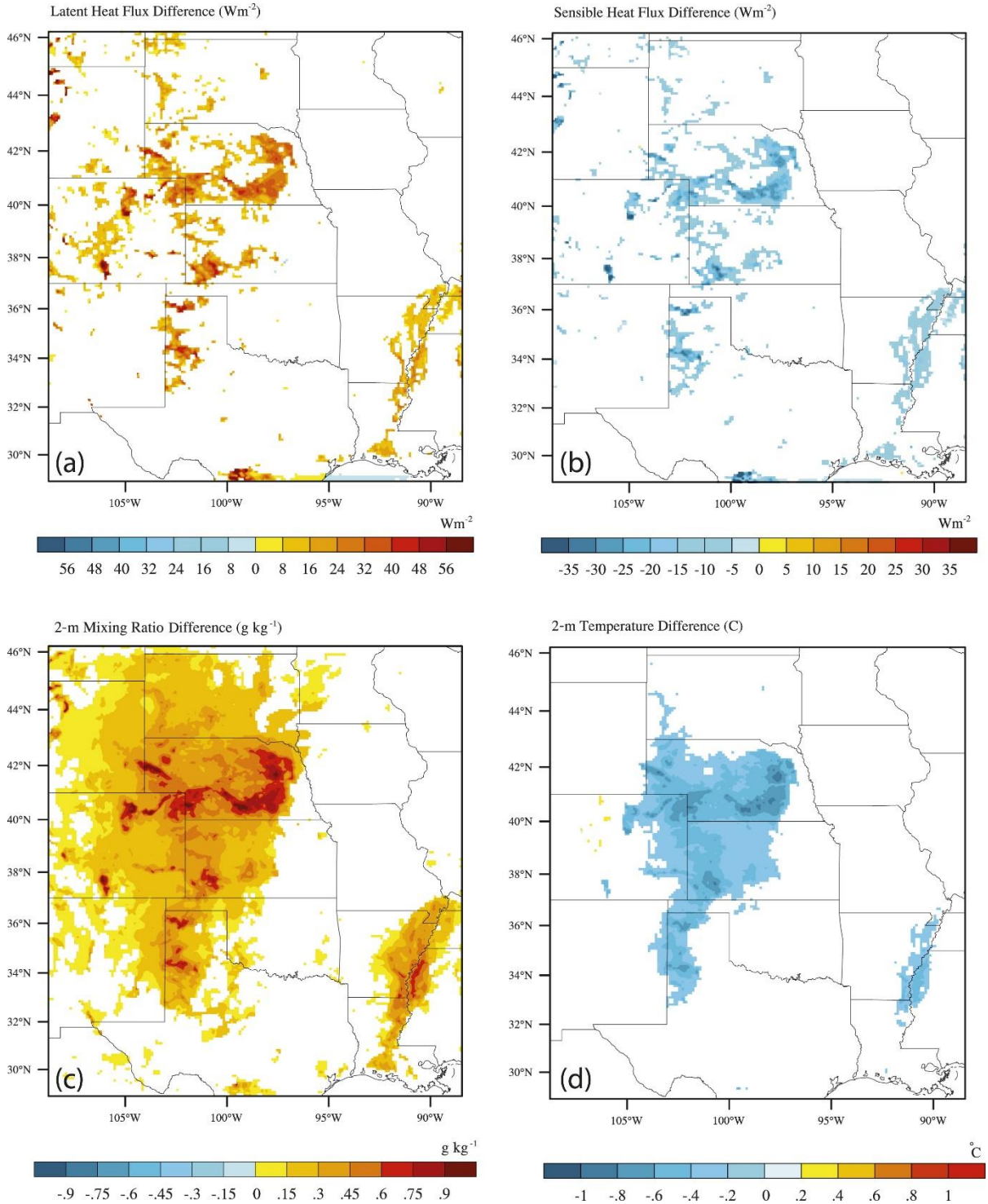

Figure 3: (a) Average May–September simulated LE difference (IRRIG minus CTRL) for all years. (b) As in (a), but for H (W m−2). (c) As in (a), but for 2-m mixing ratio (g kg−1). (d) As in (a), but for 2-m temperature (°C). Differences are shown for grid cells found to be significant using a two-tailed, paired t test at the 95% confidence level (Harding & Snyder, 2012).

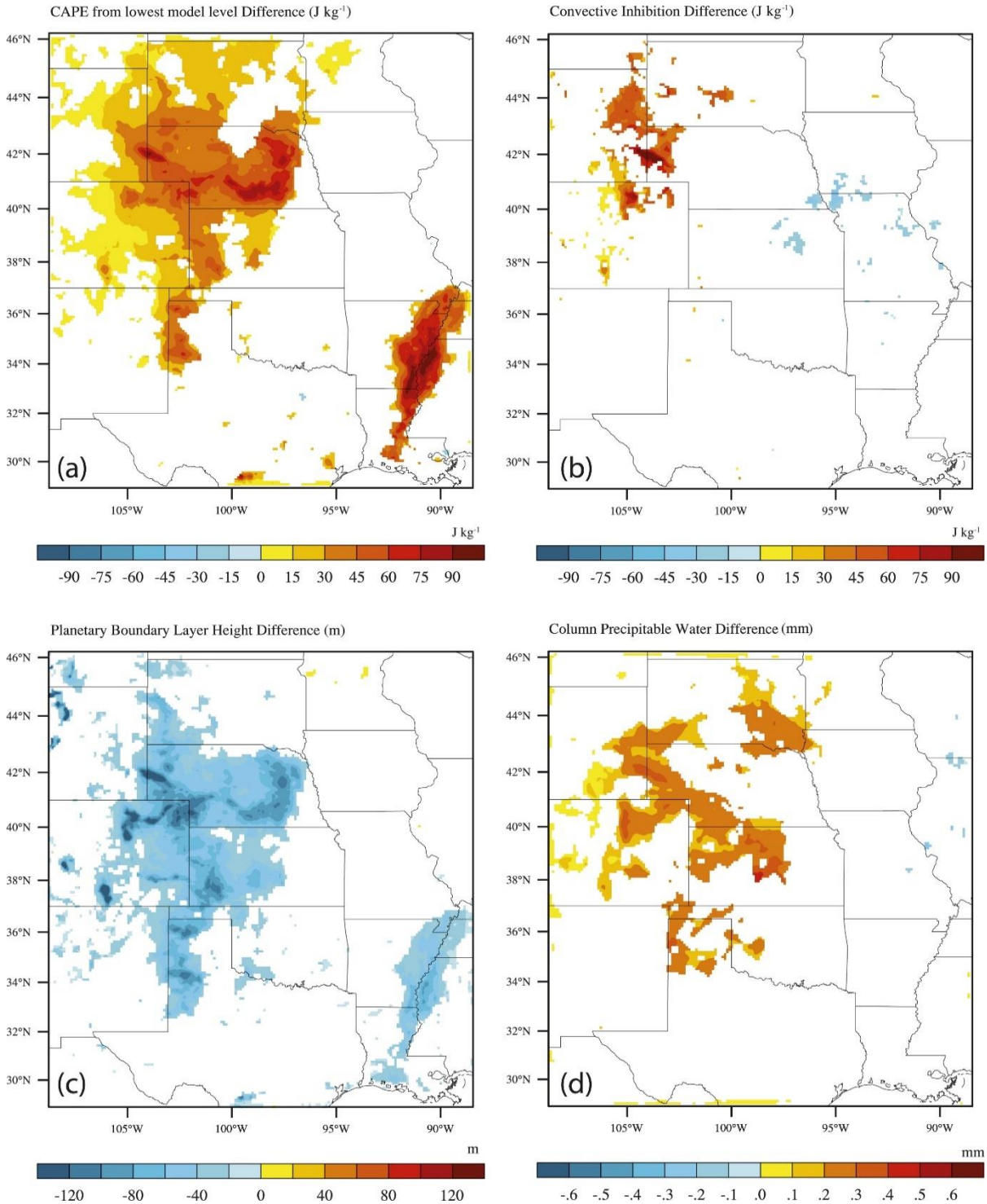

Figure 4: (a) Average May–September simulated CAPE (J kg−1) difference (IRRIG minus CTRL) for all years. (b) As in (a), but for CIN (J kg−1). (c) As in (a), but for PBL height (m). (d) As in (a), but for column precipitable water (mm). Differences are shown only for grid cells found to be significant using a two-tailed, paired t test at the 95% confidence level (Harding & Snyder, 2012).

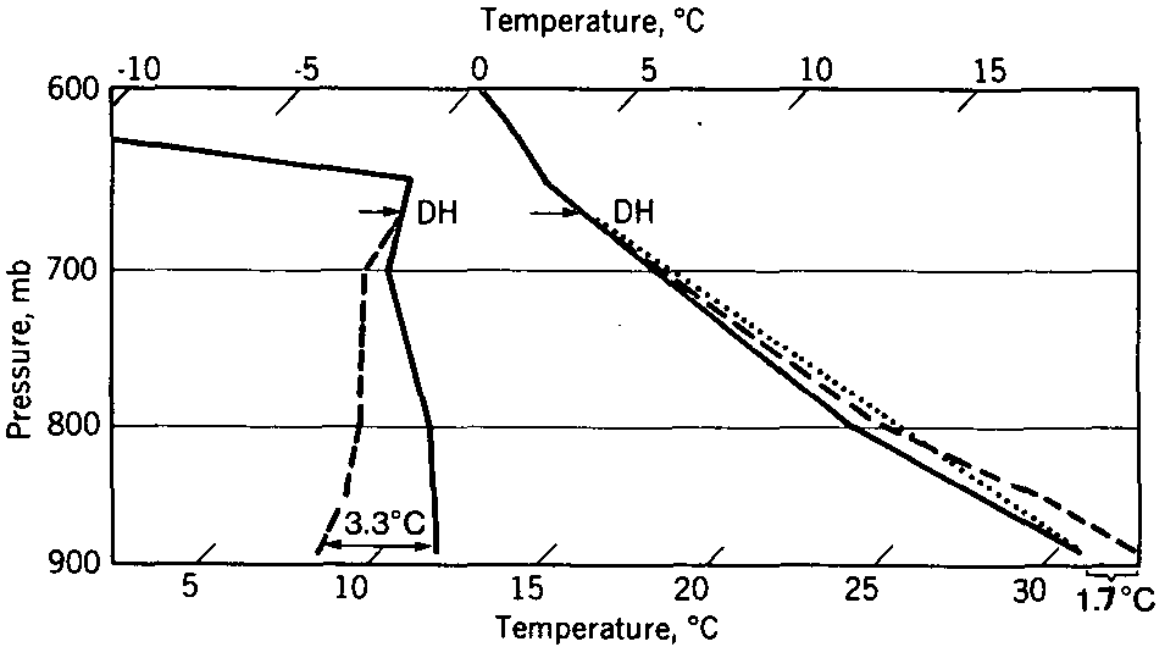

Figure 5: Sounding with dew point and temperature without irrigation (hypothetical) (dashed lines) and with irrigation (solid lines). The dotted line is the dry adiabat from which the destination height DH of an unstable, unsaturated surface parcel was determined. These lines converge to the observed soundings at DH, simulating a dry adiabatic ascent. (Barnston & Schickedanz, 1984)

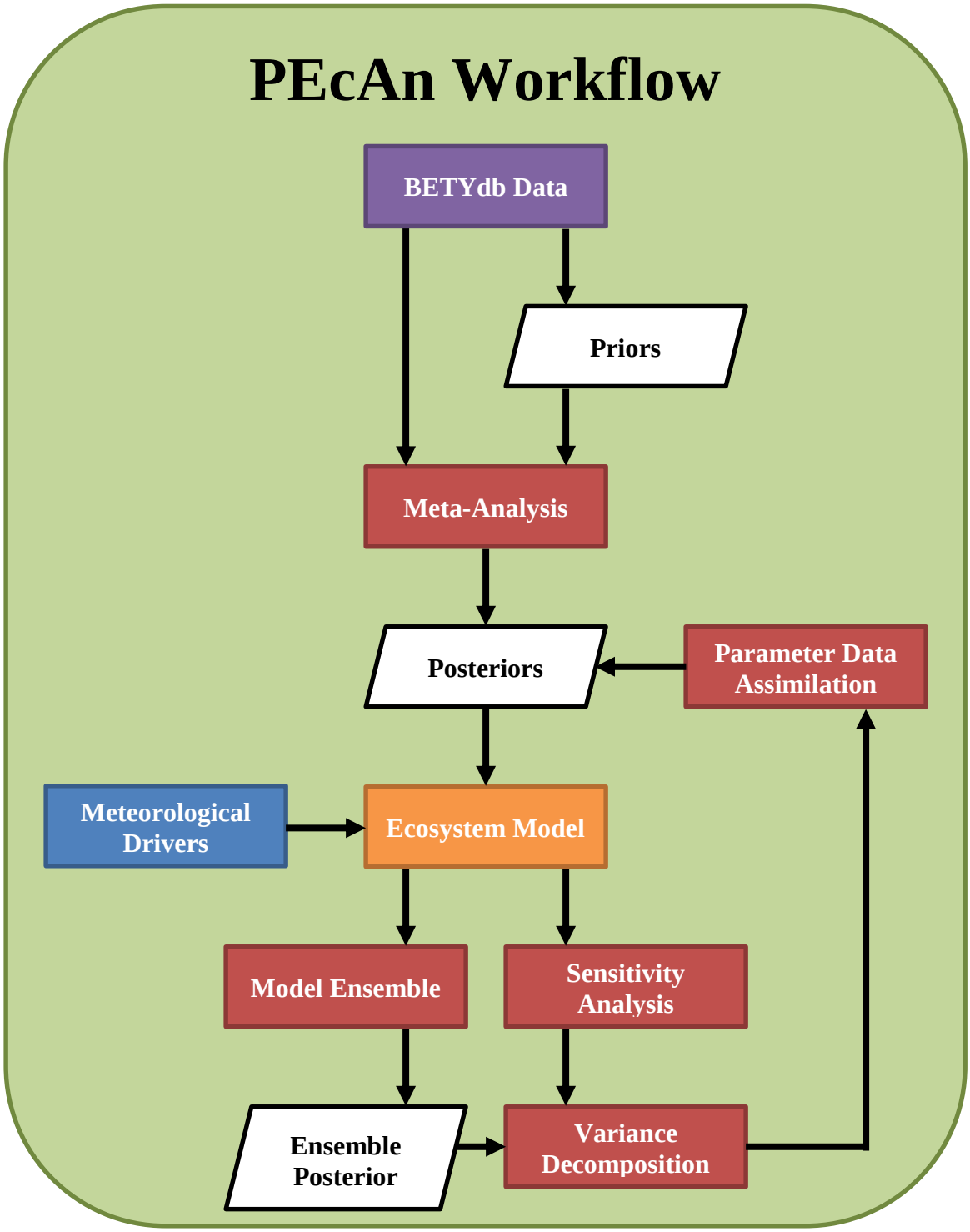

Figure 6: PEcAn workflow based off LeBauer et al. (2013). PEcAn controls the flow of information (white) through a series of modules and data analysis packages (red) between the meteorological drivers (blue), the plant trait data base BETYdb (purple), and the ecosystem model (orange).

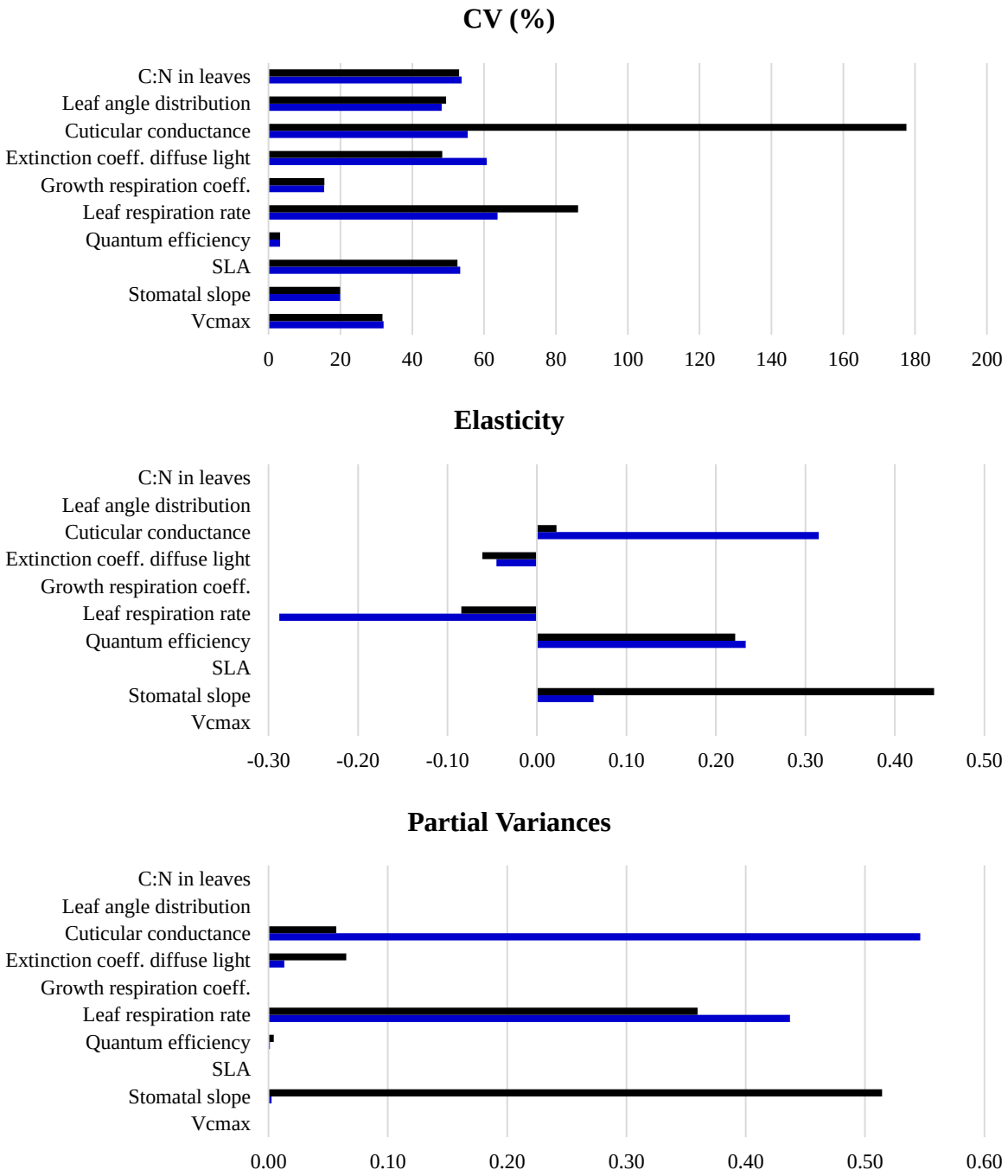

Figure 7: Partitioning of variance by parameter results from variance decomposition of default parameters (black) and post-PDA adjusted parameters (blue). Where coefficient of variation (CV) is the uncertainty associated with each parameter, where the higher the CV the higher the uncertainty. Elasticity is the sensitivity of modeled LE to each parameter, where an elasticity of 1 indicates that model parameter will double when the parameter value doubles. The variance is the contribution of uncertainty of model output of LE as a function of both the parameter uncertainty and sensitivity.

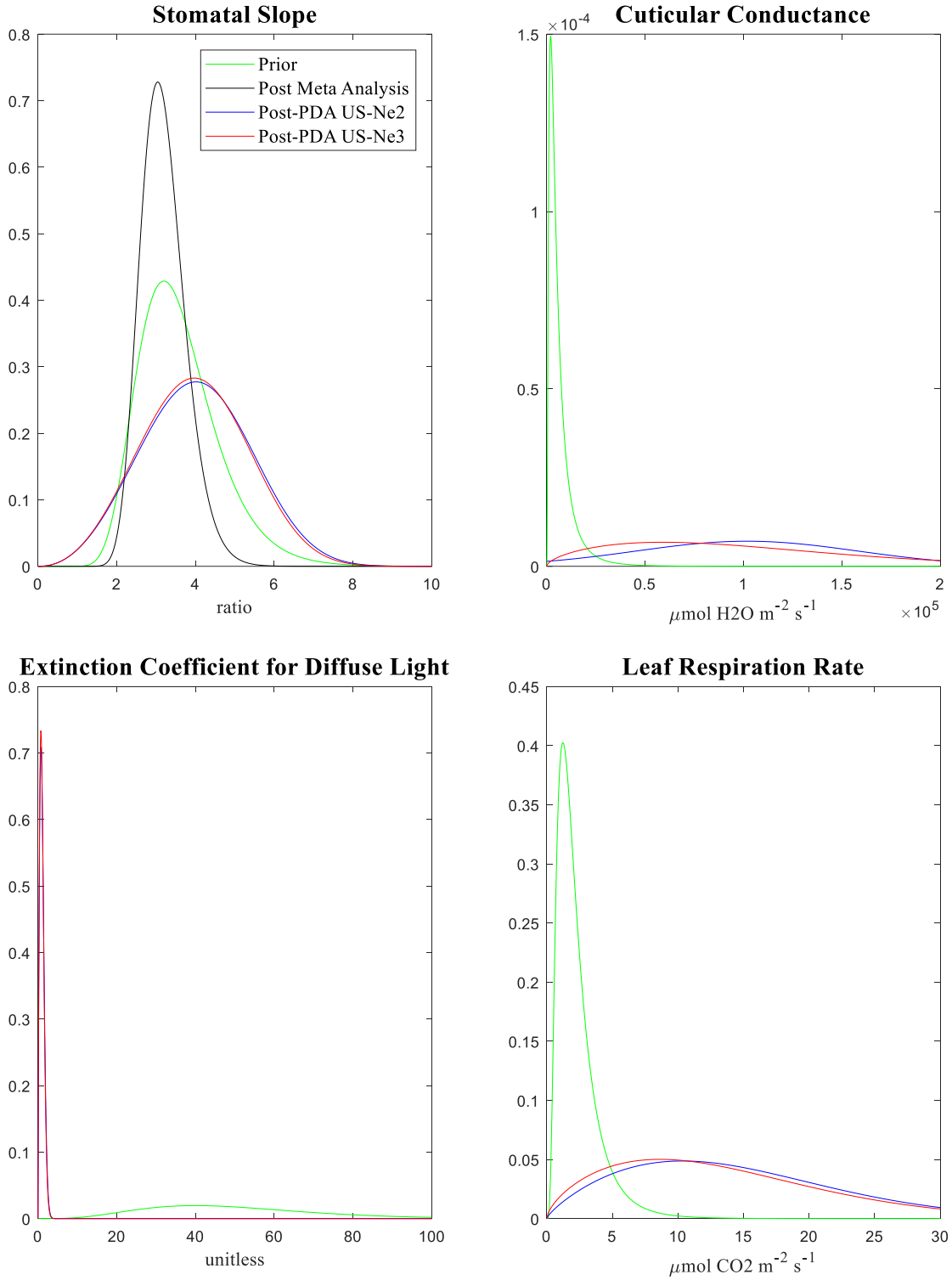

Figure 8: Probability distribution functions for stomatal slope, cuticular conductance, extinction coefficient for diffuse light, and leaf respiration rate for the default prior values (green), post meta-analysis (black), post-PDA for US-Ne2 (blue) and US-Ne3 (red).

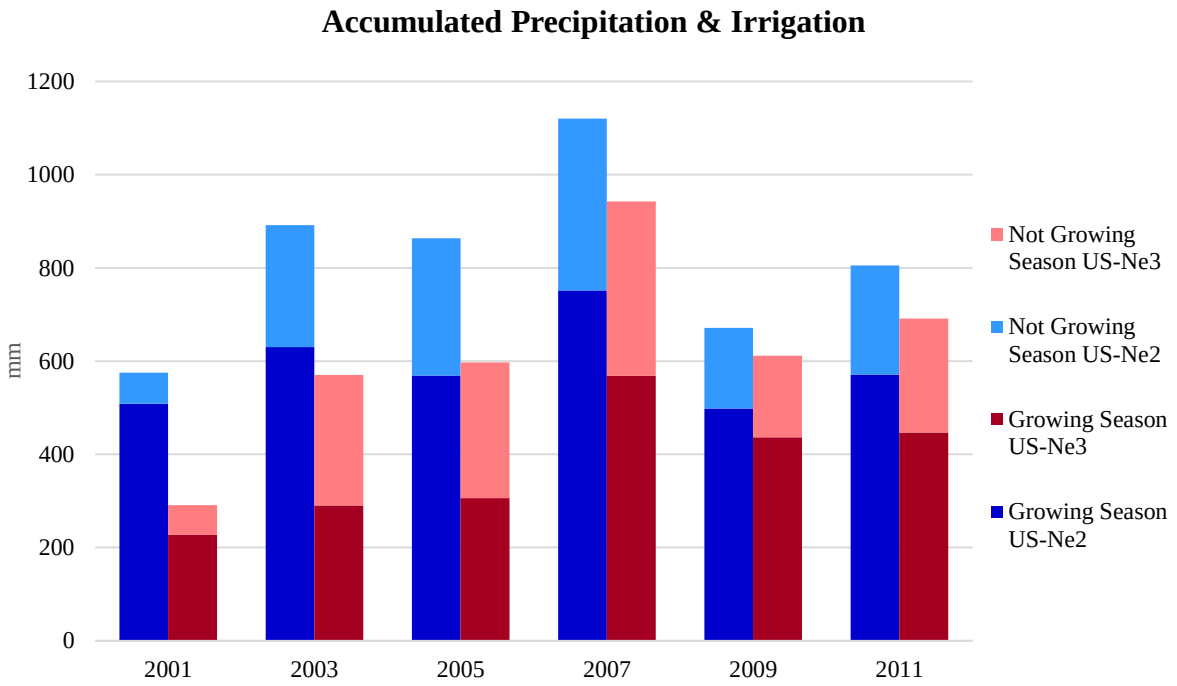

Figure 9: Annual accumulated precipitation and irrigation (mm) at the irrigated site US-Ne2 (blue) and annual accumulated precipitation (mm) at the rain-fed site US-Ne3 (red) for years when corn was growing with the darker colors represent the growing season and the pastel color is for the measured precipitation not in the growing season.

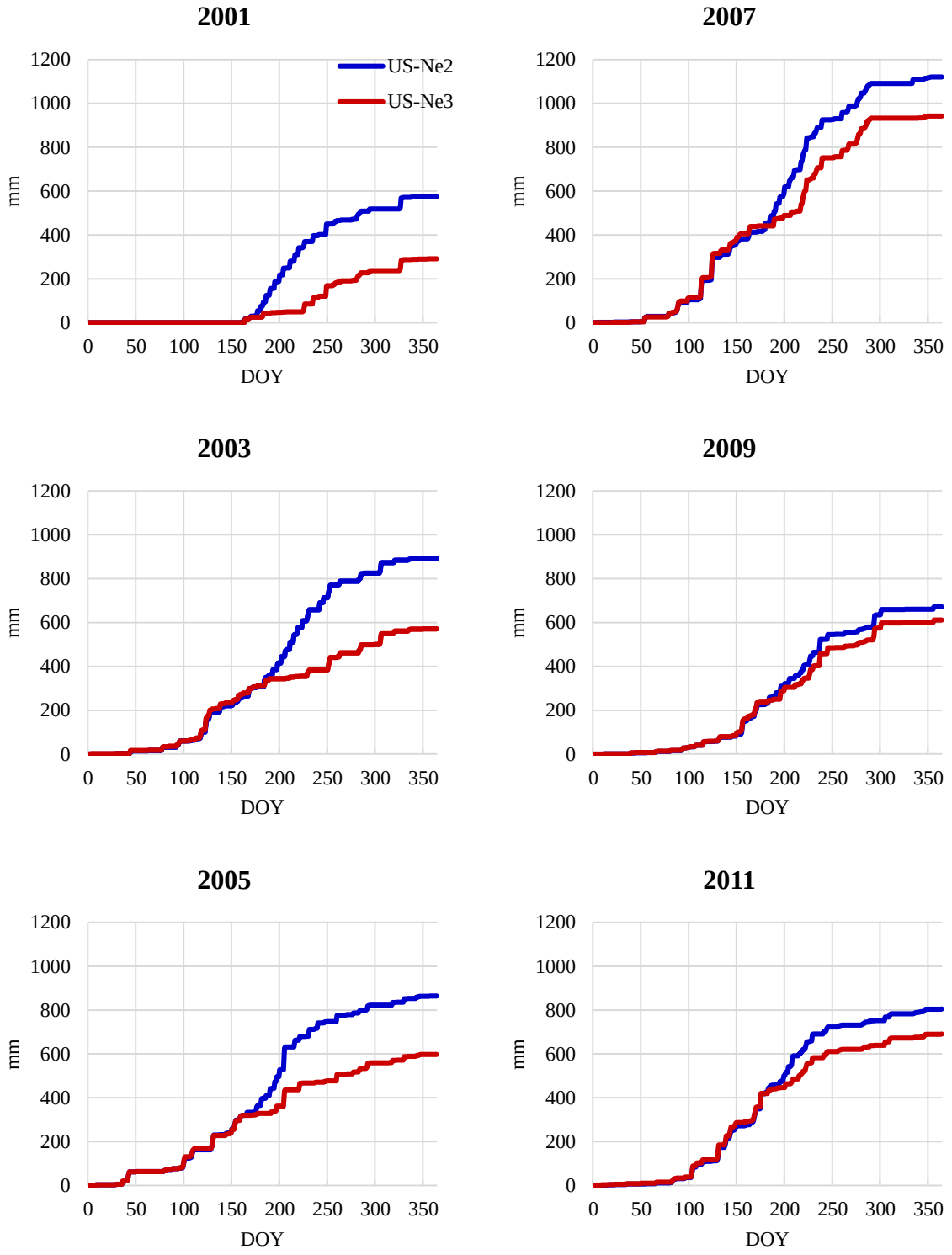

Figure 10: Daily accumulated precipitation (mm) at US-Ne3 (red) and daily accumulated precipitation and irrigation at US-Ne2 (blue) and for the corn growing years where the year 2001 had missing data for the beginning of the year.

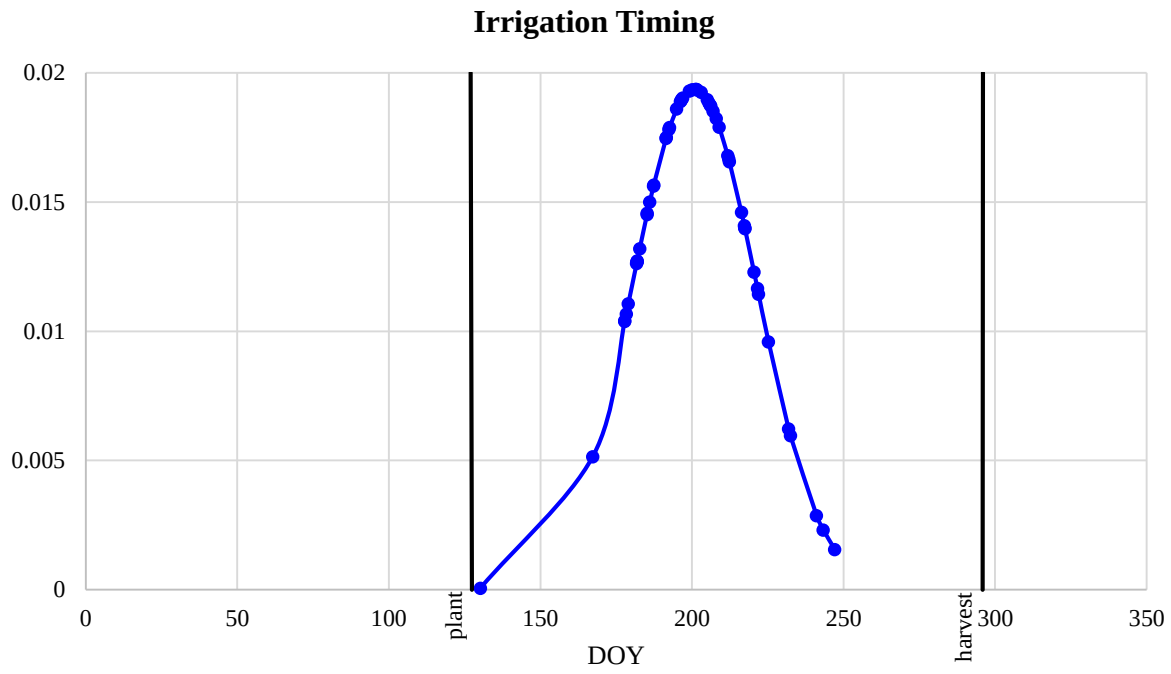

Figure 11: Probability density function of irrigation occurrences marked with blue dots for the day of year (DOY) for the corn growing years of 2001, 2003, 2005, 2007, 2009, and 2011 with the mean planting and harvest dates for corn reported at those sites in the black lines.

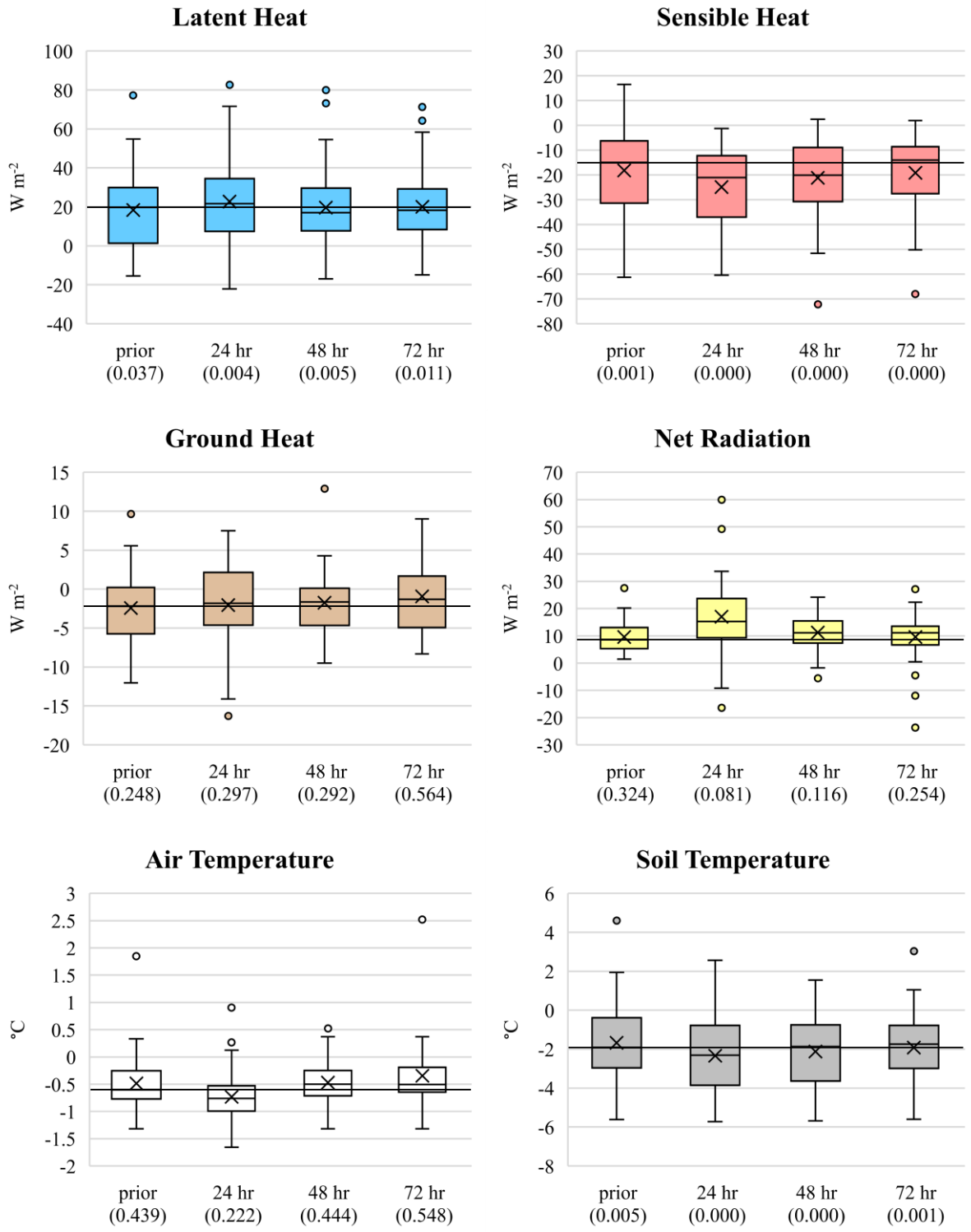

Figure 12: The difference in the 24-hour mean from US-Ne2 and US-Ne3 the day prior to irrigation, one, two, and three days after irrigation for LE, H, G, RNET, TA, and TS for the years when corn was growing. The black line represents the prior 24-hour median.

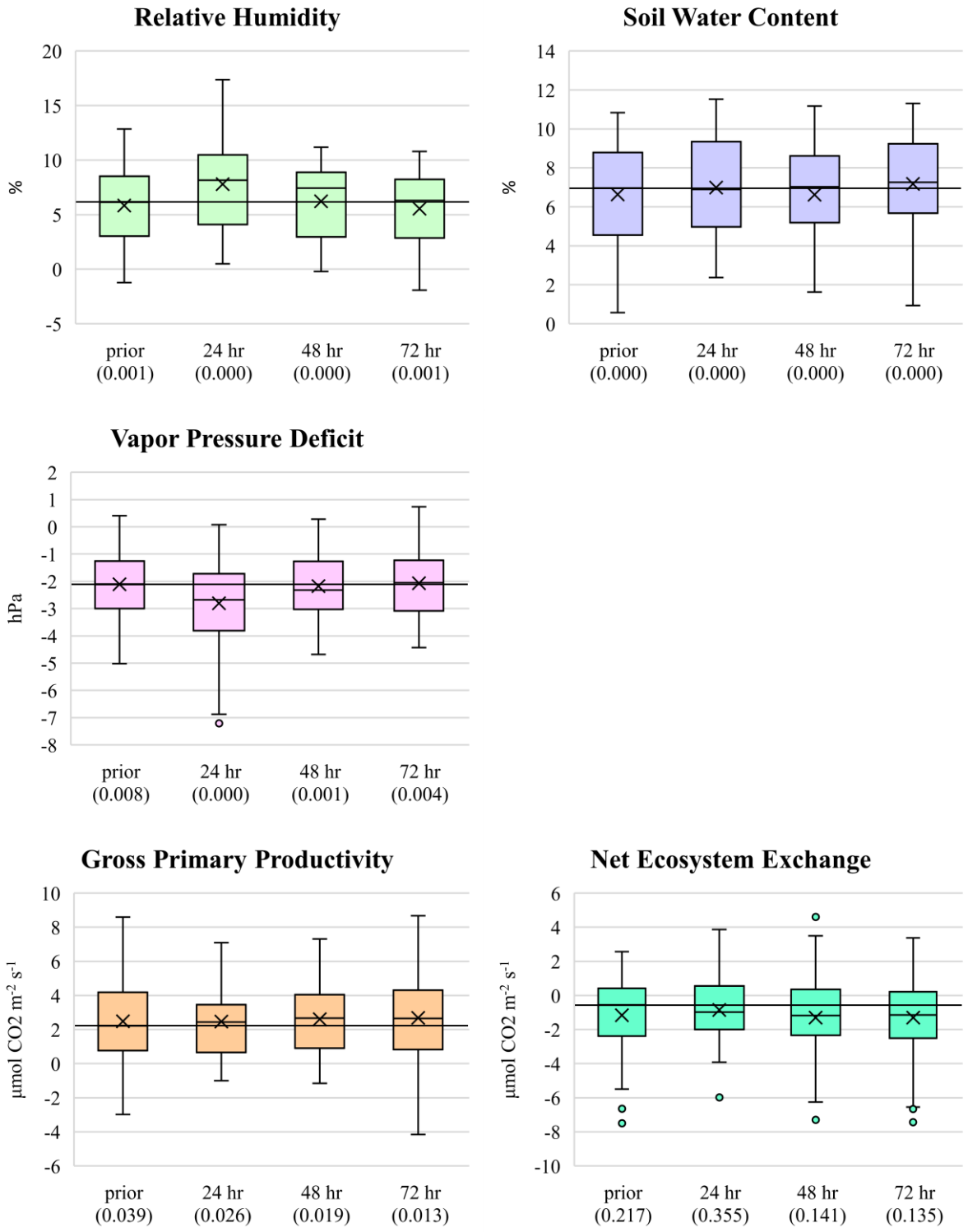

Figure 13: Same as in but for RH, SWC, VPD, GPP, and NEE.

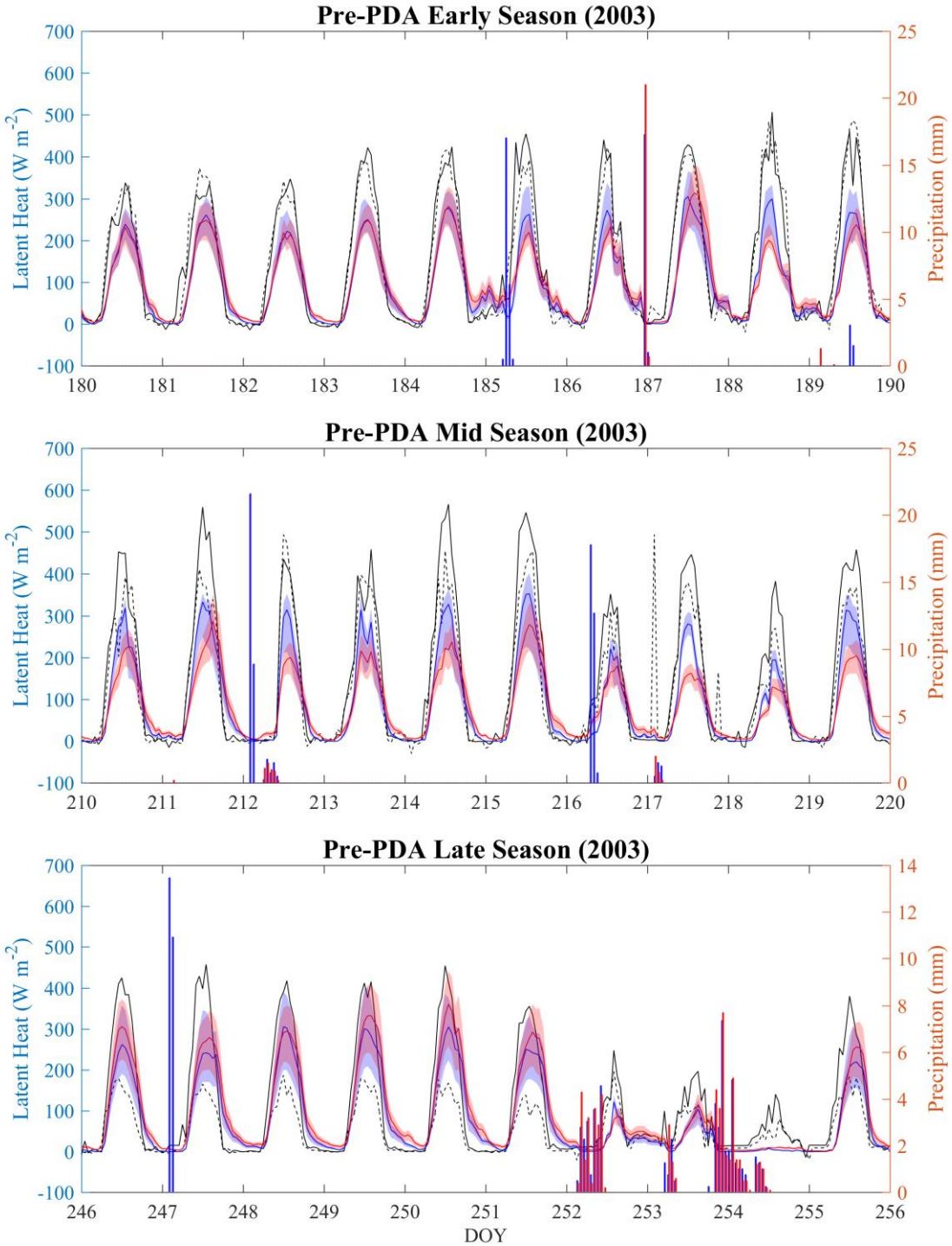

Figure 14: Observed latent heating (W m^{-2}) at US-Ne2 (solid black) and US-Ne3 (dashed black) compared with the pre-PDA model ensemble mean in blue (US-Ne2) and red (US-Ne3) and 2.5 to 97.5% confidence interval in their respective color shaded fill with the observed rainfall (red bar) and irrigation + rainfall (blue bar) in mm for a 10-day period in the early (top), mid (middle), and late (bottom) growing season of 2003.

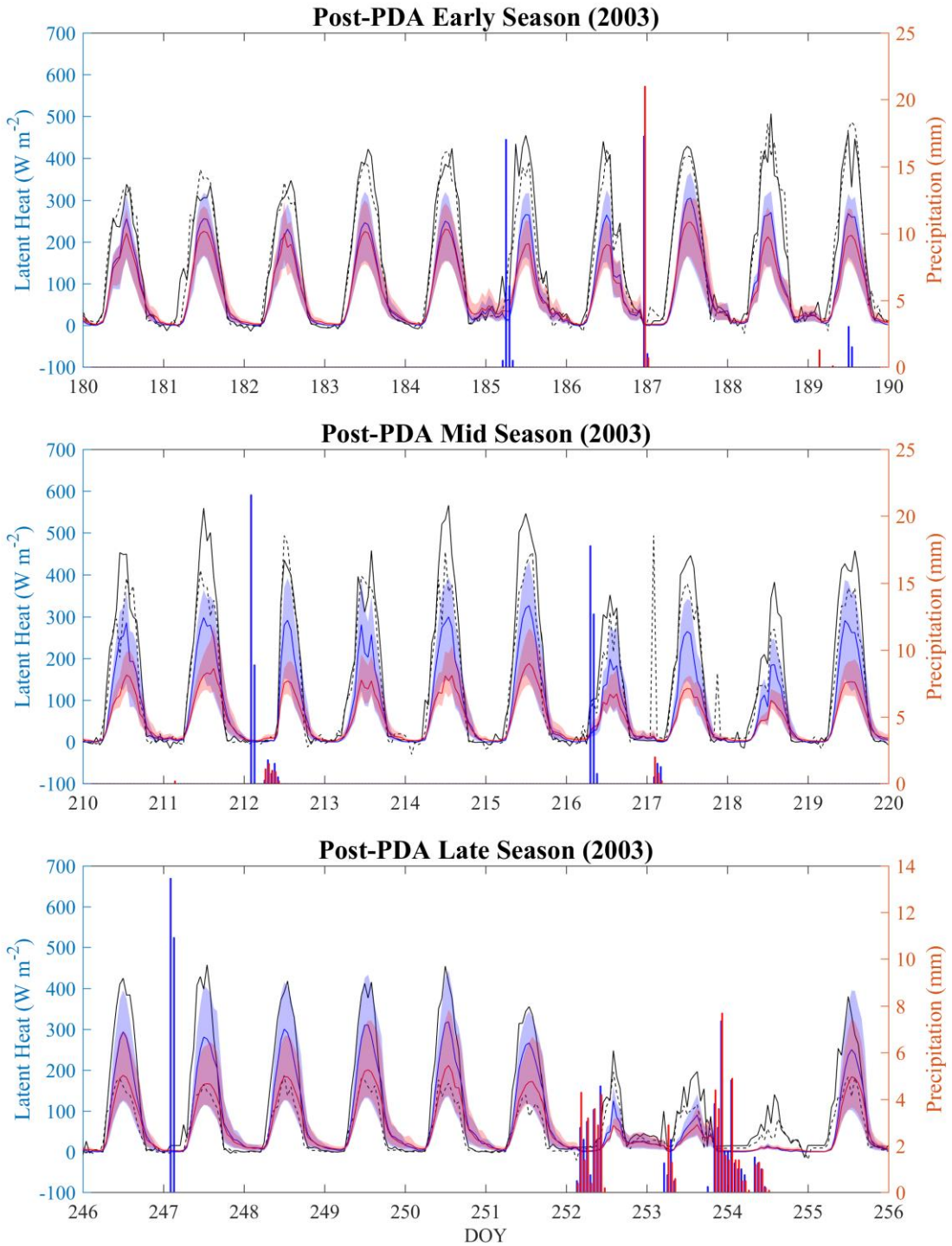

Figure 15: Like Figure 14 but for the post-PDA ensemble model runs.

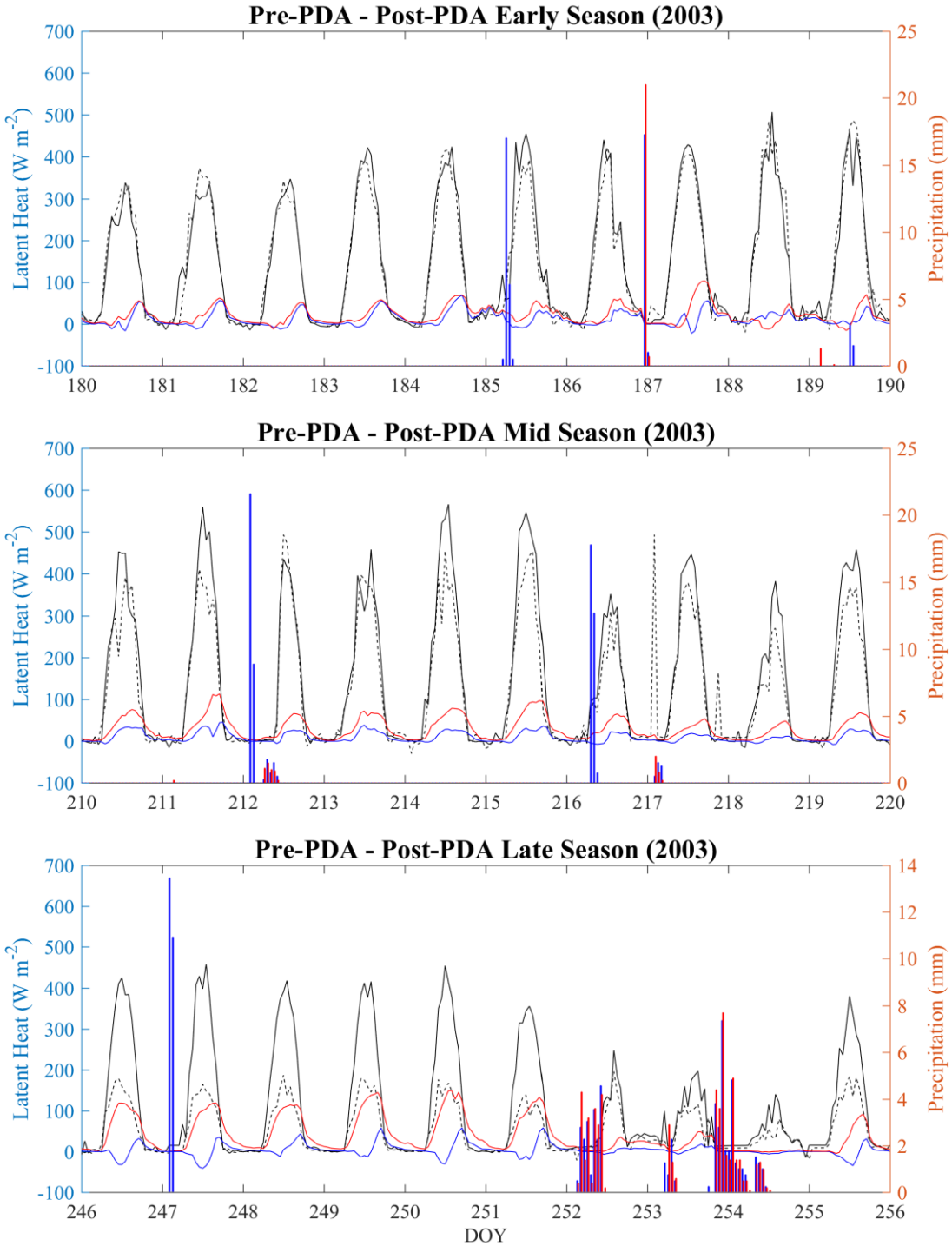

Figure 16: Same observations of latent heating and precipitation as in Figure 14 and Figure 15, but the blue line represents the pre-PDA minus post-PDA ensemble mean for US-Ne2 (blue line) and similarly for US-Ne3 (red line).

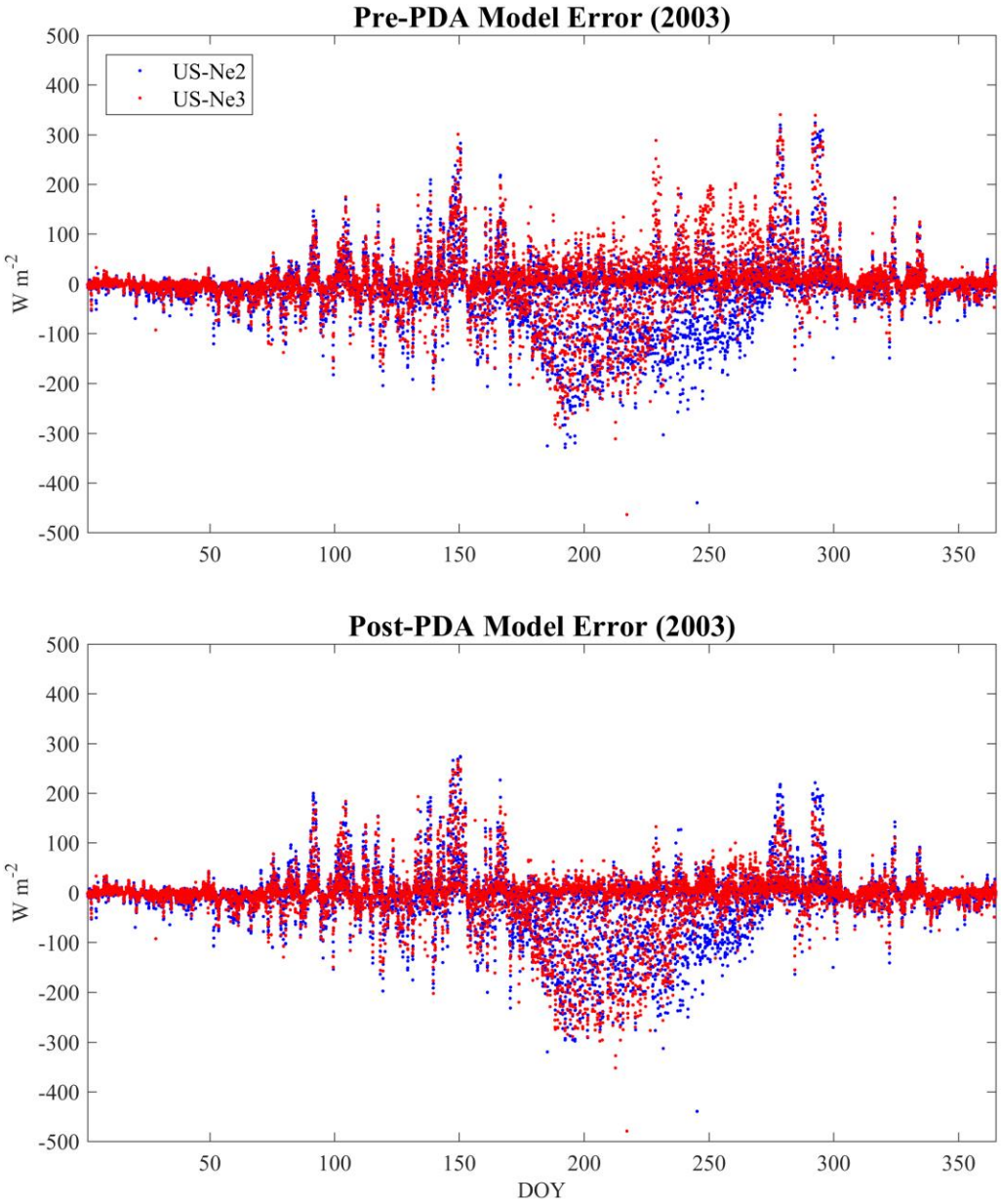

Figure 17: Model error (mean model ensemble – observations) pre-PDA (top) and post-PDA (bottom) for the year 2003 of LE at US-Ne2 (blue) and US-Ne3 (red).

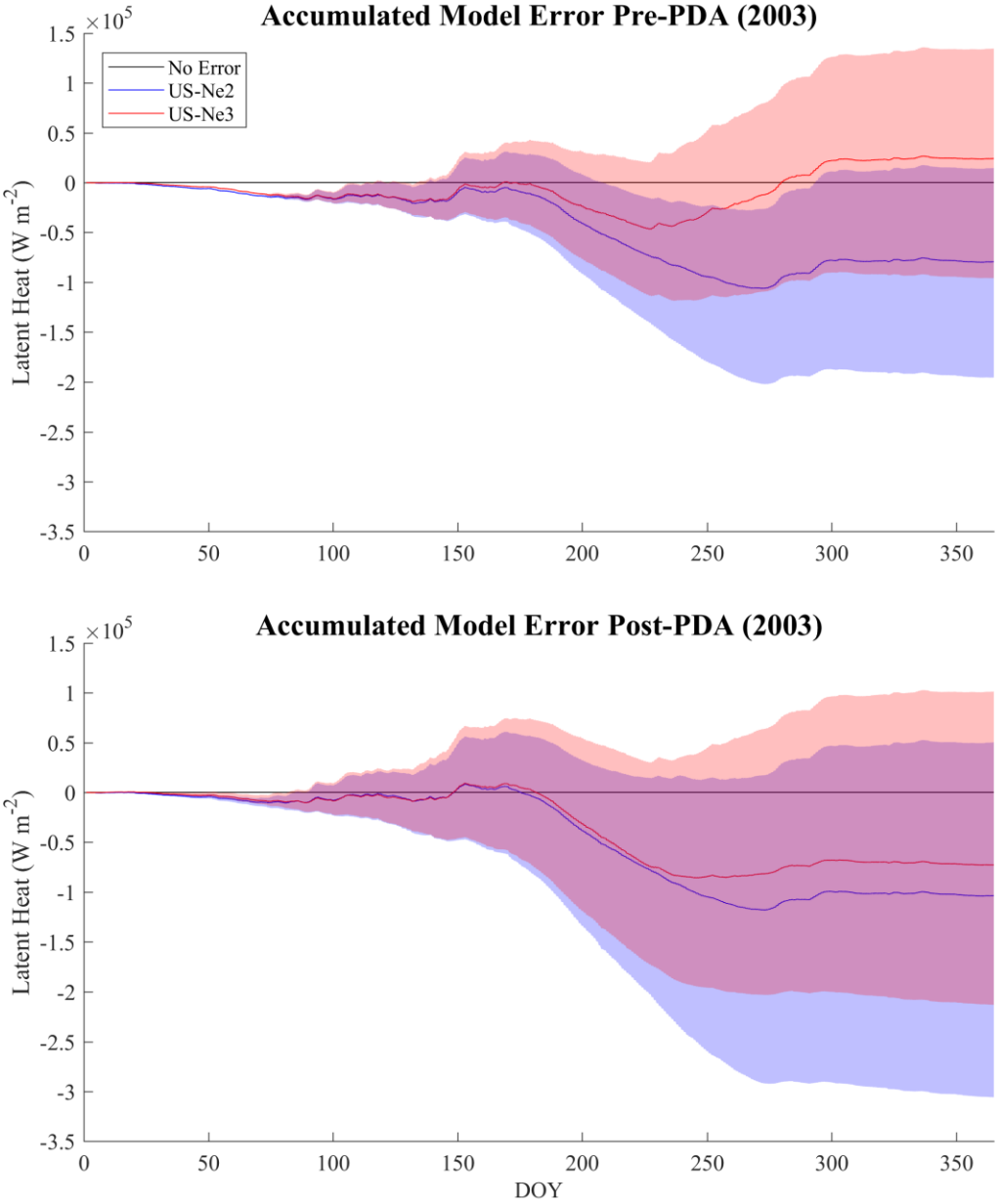

Figure 18: Accumulated model error for pre-PDA (top) and post-PDA (bottom) for the year 2003 at US-Ne2 (blue) and US-Ne3 (red) with the 2.5 to 97.5% confidence interval in the respective sites shaded color where the black line represents no error between model and observations.

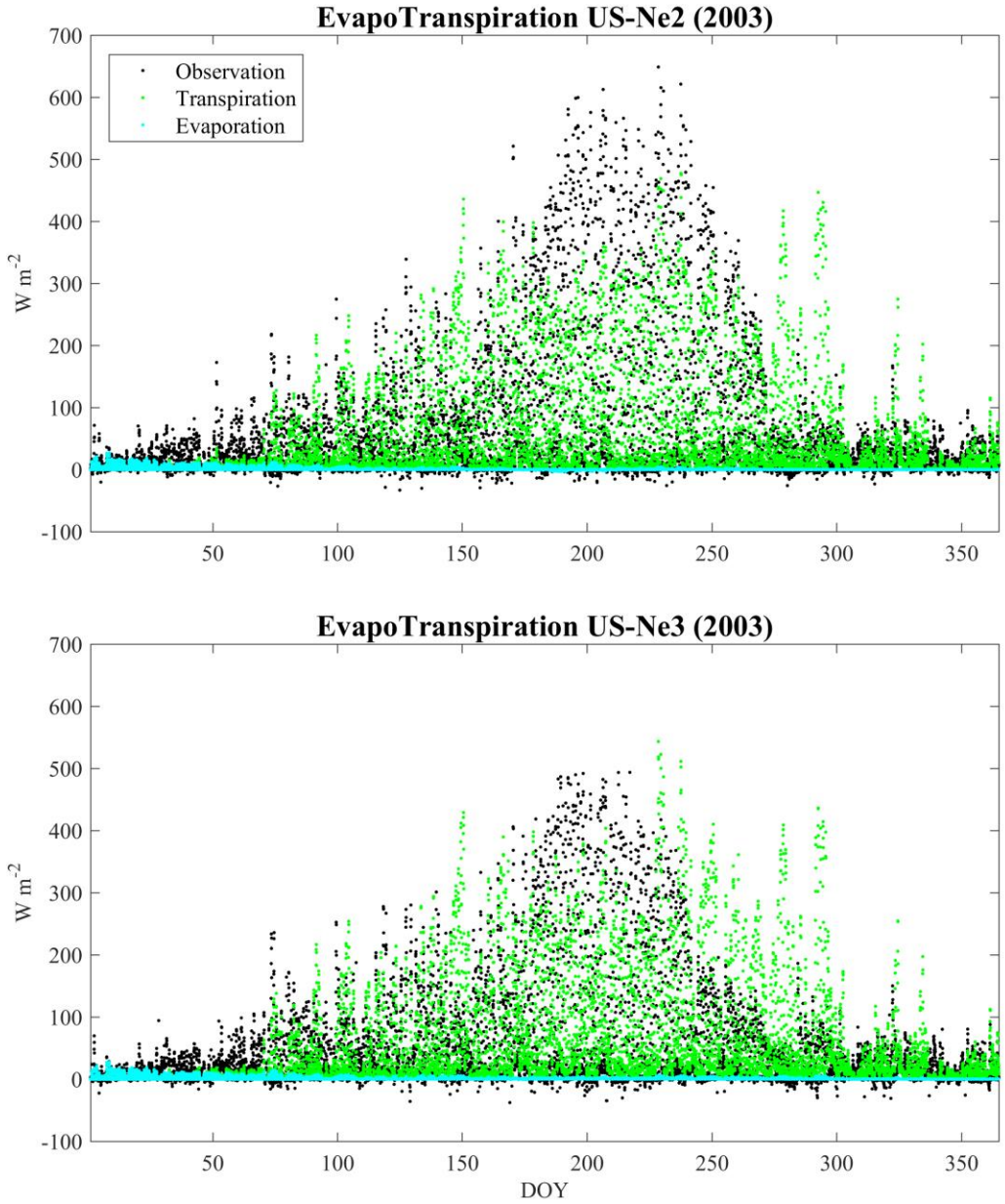

Figure 19: Hourly observations of LE (black) and pre-PDA ensemble mean of transpiration (green) and evaporation (cyan) for the year 2003 at US-Ne2 (top) and US-Ne3 (bottom).

Tables

Table 1: The parameters' post meta-analysis distributions used in model parameterization. Columns A and B represents mean and standard deviation respectively for normal and log normal distributions, shape and scale parameters respectively for the gamma and Weibull distributions, and the first and second shape parameters respectively for the Beta distribution. The column N represents the number of observations, phylogeny is the group of plants that the trait was observed for, and source is where the observations originally came from. The italicized rows represent the parameters that were chosen for the parameter date assimilation.

Parameter (units)	Distribution	A	B	N	Phylogeny	Source
C:N in leaves (ratio)	Gamma	4.18	0.13	95	Grass	Wright et al. 2004
Cuticular Conductance ($\mu mol\ H2O\ m^{-2}\ s^{-1}$)	*Log normal*	*8.4*	*0.9*	-	*All plants*	*LeBauer 2010 **
Extinction Coefficient for Diffuse Light (unitless)	*Gamma*	*5*	*10*	-	*plants*	-
Growth Respiration Coefficient (mol CO2 per mol net assimilation)	Beta	26	48	-	plants	LeBauer 2010 *
Leaf Angle Distribution (ratio)	Log normal	0.18	0.43	10	grass	Campbell & Norman 1998
Leaf Respiration Rate ($\mu mol\ CO2\ m^{-2}\ s^{-1}$)	*Log normal*	*0.632*	*0.65*	*32*	*Graminoid*	*LeBauer 2010 **
Quantum Efficiency (fraction)	Normal	0.059	0.002	16	Maize	BETYdb †
Specific Leaf Area ($m^2\ kg^{-1}$)	Weibull	2.06	19	125	grass	Wright et al. 2004
Stomatal Slope (ratio)	*Log normal*	*1.144*	*0.177*	*1*	*Maize*	*BETYdb †*
Vmax ($\mu mol\ CO2\ m^{-2}\ s^{-1}$)	Log normal	3.75	0.3	12	Monocot Ag crops	Wullschleger et al. 1993

* Expert prior knowledge

† Maize specific measurements post meta-analysis distributions

Table 2: The parameters selected for parameter data assimilation as previously described in Table 1. The pre-PDA and post-PDA parameter distributions for US-Ne2 and US-Ne3 as graphed in Figure 8.

Parameter	Cuticular Conductance	Extinction Coefficient for Diffuse Light	Leaf Respiration Rate	Stomatal Slope
Pre-PDA Distribution	Log Normal	Gamma	Log Normal	Log Normal
A	8.4	5	0.632	1.24
B	0.9	10	0.65	0.28
US-Ne2 Post-PDA Distribution	Normal	Weibull	Weibull	Weibull
A	101765.3	1.8483	1.7822	3.2162
B	56443.51	1.15	16.4322	4.5059
US-Ne3 Post-PDA Distribution	Weibull	Weibull	Weibull	Weibull
A	1.5767	1.8548	1.6388	3.2419
B	111752.2	1.1145	15.3456	4.4458

Table 3: Growing season hourly averages of the observations at the site US-Ne2, US-Ne3, the difference between US-Ne2 and US-Ne3, and the probability value for all the corn growing years with the year 2001 having observations start on the 166th DOY.

Observed Variable (units)	**US-Ne2**	**US-Ne3**	**Δ**	**P-value**
LE (W m^{-2})	99.10	86.25	12.85	0.000
H (W m^{-2})	16.48	29.14	-12.66	0.000
G (W m^{-2})	3.95	4.84	-0.89	0.160
RNET (W m^{-2})	145.84	137.48	8.36	0.001
TA (°C)	20.79	21.16	-0.37	0.118
TS (°C)	20.75	21.64	-0.90	0.000
RH (%)	76.23	71.19	5.04	0.000
SWC (%)	35.04	30.40	4.65	0.000
VPD (hPa)	7.29	8.81	-1.52	0.000
GPP (µmol CO2 m^{-2} s^{-1})	11.76	10.14	1.62	0.000
NEE (µmol CO2 m^{-2} s^{-1})	-5.29	-4.49	-0.80	0.007

Table 4: Maximum LAI, height, and yield at US-Ne2 and US-Ne3 for the following years.

Year	Site	Max LAI (m^2 m^{-2})	Max Height (m)	Yield (Mg ha^{-1})
2001	US-Ne2	6.08	3.43	13.41
2001	US-Ne3	3.88	2.66	8.72
2003	US-Ne2	5.53	2.89	14.00
2003	US-Ne3	4.27	2.50	7.72
2005	US-Ne2	4.84	2.70	13.21
2005	US-Ne3	4.33	2.56	9.10